AIMS Mathematics

https://www.aimspress.com/journal/Math

AIMS Mathematics, 9(8): 20014–20042.
DOI:10.3934/math.2024976
Received: 26 March 2024
Revised: 06 June 2024
Accepted: 12 June 2024
Published: 20 June 2024

*Research article*

# Stability and bifurcation analysis of a discrete-time plant-herbivore model with harvesting effect

**Mohammed Alsubhi[1], Rizwan Ahmed[2], Ibrahim Alraddadi[3,*], Faisal Alsharif[1] and Muhammad Imran[2]**

[1] Department of Mathematics, College of Science, Taibah University, Al-Madinah Al-Munawarah, Saudi Arabia
[2] Department of Mathematics, Air University Multan Campus, Multan, Pakistan
[3] Department of Mathematics, Faculty of Science, Islamic University of Madinah, Madinah, Saudi Arabia

* **Correspondence:** Email: ialraddadi@iu.edu.sa.

**Abstract:** The dynamics of plant-herbivore interactions are essential for understanding ecosystem stability and resilience. This article investigated the effects of incorporating a harvesting effect on the dynamics of a discrete-time plant-herbivore system. An analysis was performed to determine the existence and stability of fixed points. In addition, studies have shown that the system experienced transcritical, period-doubling, and Neimark-Sacker bifurcations. Moreover, we provided numerical simulations to substantiate our theoretical results. Our research indicated that harvesting in excessive amounts may have negative effects on the populations of both plants and herbivores. However, when harvesting was done at moderate levels, it promoted the coexistence and stability of both populations. The findings of our analysis provided a deep understanding of the intricate dynamics of ecological systems and underscored the need to use sustainable harvesting methods for the management and preservation of ecosystems.

**Keywords:** plant-herbivore system; harvesting effect; local stability analysis; local bifurcation analysis; computational analysis
**Mathematics Subject Classification:** 39A28, 39A30

## 1. Introduction

A plant-herbivore system is an ecological interaction in which plants function as main producers and herbivores consume them as their major source of living. The creation of this connection is vital for the efficient operation of the ecosystem and the conservation of biodiversity. Plants use photosynthesis to capture solar energy and convert it into organic matter. They serve as the fundamental basis of food webs, providing herbivores and other trophic levels with the energy and nutrition they need to survive. Herbivores are living things that eat plant tissues such as leaves, stems, fruits, and roots. Plant-herbivore interactions have a profound influence on ecosystem processes and resources. It appears that variations in the number of plants may have a substantial impact on the cycling of nutrients, the structure of the soil, and the availability of habitat, which in turn can have an effect on the abundance and distribution of other organisms within the ecosystem. Herbivores, in addition to being prey for predators, have the ability to impact the interactions that occur between predators and prey, as well as the trophic cascades that occur between different groupings of animals. The interaction between plants and herbivores is a fascinating and nuanced element of ecology, characterized by complex, frequently nonlinear relationships that may result in threshold effects. Minor changes on small scales may have significant implications on bigger scales [1–4]. Plant-herbivore interactions are important, but their dynamics may be challenging to understand due to complex ecological relationships [5–11].

Plant-herbivore interactions are often described through modified versions of predator-prey models due to their similar dynamics and ecological principles. Both types of models aim to represent the relationships between predators (also known as herbivores) and their prey (also known as plants) at different trophic levels within an ecosystem. Although plant-herbivore interactions and predator-prey interactions have certain similarities, such as population control and feeding relationships, there are key differences that arise from the unique behaviors of each kind of interaction. In the context of plants and herbivores, there is no occurrence of a predator (herbivore) chasing its victim (plant) [12]. Contrary to predators, herbivores do not engage in the aggressive pursuit or killing of plants. Herbivory, on the other hand, refers to consuming leaves, stems, fruits, or roots using specialized mouthparts or feeding structures to obtain nutrients from plant tissues.

Various studies have explored the qualitative behavior of plant-herbivore models, examining phenomena such as bistability, bifurcations, and chaos control. These investigations have provided valuable insights into the dynamic complexities of plant-herbivore interactions, contributing to our understanding of ecosystem dynamics. Researchers have investigated plant-herbivore interactions using both continuous-time differential equations and discrete-time difference equations. Kartal [13] investigated the dynamical behavior of a plant-herbivore system, including both differential and difference equations. Beso et al. [14] investigated stability and various types of bifurcations in a plat-herbivore system with a strong Allee effect. Din [15] investigated the global behavior of a discrete-time plant-herbivore system. Khan et al. [16] conducted bifurcation analysis of a discrete-time plant-herbivore system. Hamada [17] investigated stability, bifurcation, and chaos in a discrete-time plant-herbivore system obtained from a continuous-time plant-herbivore system by applying the piecewise constant argument method. Similarly, for some other discussions related to the population dynamics of plant-herbivore systems, we refer the interested reader to [18–23] and references therein.

The apple twig borer (ATB), a pest infesting grapevines, serves as a case study illustrating the ecological dynamics of plant-herbivore systems. Previous studies [24, 25] proposed fundamental frameworks based on the life cycle of adult ATBs, laying the groundwork for understanding the dynamics of plant-herbivore interactions. Understanding these dynamics is crucial for land management, environmental protection, and animal husbandry, prompting extensive research into dynamical system models to elucidate population and ecosystem behaviors. In [11], Din et al. investigated the stability, Neimark-Sacker bifurcation, and chaos in the following discrete-time plant-herbivore system with Holling type-II functional response:

$$\begin{cases} x_{n+1} = \frac{x_n}{r(1+y_n)+\kappa x_n}, \\ y_{n+1} = \sigma(1+x_n)y_n, \end{cases} \tag{1.1}$$

where $x_n$ and $y_n$, respectively, represent the population densities of grapevine and ATB. Moreover, $r$, $\kappa$, and $\sigma$ are positive constants.

In population dynamics, harvesting refers to the intentional removal of individuals from a population for human use or consumption. This practice is common in various natural resource management contexts, including fisheries [26,27], forestry [28,29], and wildlife management [30–32]. Harvesting may be detrimental to the health of ecosystems and biodiversity if it is carried out in an excessive or indiscriminate manner. Understanding the consequences of such efforts is necessary for the implementation of sustainable management systems. Within the framework of plant-herbivore interactions, the act of harvesting may directly influence the populations of both plants and herbivores, resulting in changes to the composition, abundance, and distribution of these populations. The harvesting of plants has the potential to reduce population densities, disrupt reproductive cycles, and alter the structure of communities by favoring some species over others. There is also the possibility that these effects might occur simultaneously. Similarly, herbivores may experience changes in population dynamics, resource availability, and foraging behavior as a result of the pressure exerted by harvesting. Furthermore, the removal of individuals from both the plant and herbivore populations has the potential to upset the delicate balance that exists between them, which may have a domino effect on higher trophic levels as well as the general functioning of the ecosystem. In the study conducted by Virtala [33], the optimum harvesting in a plant-herbivore system was investigated. The study conducted by Asfaw et al. [34] investigated a plant-herbivore system that included herbivore harvesting effects. They provided evidence that the harvest rate of the herbivore population has a significant influence on the dynamics of herbivores.

When it comes to effectively managing plant-herbivore systems, there are a few different harvesting strategies to choose from. These include proportional, constant, nonselective, and selective harvesting [35–38]. Each approach has its own set of repercussions, both for the coexistence of organisms and for the dynamics of the ecosystem. The term selective harvesting refers to a technique that focuses on certain individuals or species, taking into consideration specific characteristics such as size, age, or quality. This strategy makes it possible to exert conservation and management activities in a focused manner. In contrast, nonselective harvesting entails the extraction of individuals without taking into account their distinct features or characteristics. This might potentially have unanticipated consequences for the structure of populations and the operation of ecosystems. Constant harvesting is the consistent and regular extraction of a set quantity from a population, which consistently affects the population dynamics independent of variations in population density. In contrast, proportionate harvesting maintains a harvest rate that is directly proportional to the size of the present population, ensuring that the intensity of harvesting increases or decreases with the abundance of the population. This adaptable strategy enables flexible administration by shifting population dynamics and fostering sustainable use of resources and stability in the population. Proportionate harvesting may provide more adaptability to changes in the environment and variations in population size, especially in ecosystems that are dynamic or changing.

Therefore, inspired by the preceding discussion, we are interested to inquire: What are the consequences for the dynamic properties when a harvesting impact is applied to the plant population in system (1.1)? Therefore, we modified system (1.1) by integrating the harvesting impact into the plant population. The result is the following modified system:

$$\begin{cases} x_{n+1} = \frac{x_n}{r(1+y_n)+\kappa x_n} - hx_n, \\ y_{n+1} = \sigma(1 + x_n)y_n, \end{cases} \tag{1.2}$$

where $h > 0$ is the harvesting rate. It represents the intensity of harvesting. Ensuring nonnegative solutions is of utmost importance in ecological models, such as the plant-herbivore model, to maintain biological relevance. Negative solutions are not ecologically meaningful since populations cannot have negative densities. Ensuring solution positivity is crucial for aligning model predictions with ecological reality, which in turn facilitates the correct understanding and management of ecosystems. We assume that the initial values $x_0$ and $y_0$ are positive. Clearly, from the second equation of system (1.2), it is evident that $y_{n+1} > 0$ for all $n$. In the first equation, the term $-hx_n$ can produce negative values of $x_{n+1}$. One should select $h$ sufficiently small so that $x_{n+1}$ is positive. It can be checked that if $h$ is sufficiently small enough and $h < \frac{1}{r(1+y_0)+\kappa x_0}$, then $x_{n+1} > 0$ for all $n$. Another approach, given in Section 3.6 of [39], is that $x_{n+1}$ can be redefined as follows:

$$x_{n+1} = max\left\{0, \frac{x_n}{r(1 + y_n) + \kappa x_n} - hx_n\right\}.$$

Moreover, in all our simulations performed here, solutions remained nonnegative. Through a combination of analytical techniques and numerical simulations, we seek to address the following research questions:

- What are the effects of plant harvesting on the fixed points of the plant-herbivore system (1.2)?
- How does plant harvesting influence the stability properties of fixed points, and under what conditions do bifurcation phenomena occur?
- What insights can be gained from bifurcation analysis regarding the long-term dynamics of the modified plant-herbivore system?

For the detailed analysis of stability and bifurcation in discrete-time systems, we refer the readers to [40–44] and references therein. The subsequent sections of the paper are arranged as follows: Section 2 is dedicated to investigating the existence and stability of fixed points. Section 3 examines the study of bifurcations that include period-doubling (PD), transcritical (TC), and Neimark-Sacker (NS) occurring at the positive fixed point (FP). In Section 4, numerical simulation results are presented to support the theoretical analysis and display the new and rich dynamic behavior. Moreover, the influence of harvesting on system dynamics is presented in Section 5. Finally, a brief conclusion is presented in Section 6.

## 2. Existence and stability of FPs

Exploring the stability of FPs is very important in plant-herbivore environments. These FPs are states of equilibrium where both plant and herbivore populations are balanced. By examining their stability, we can predict long-term behavior in ecological systems, improving our understanding of the multiple components that affect ecosystem dynamics.

*2.1. Existence of FPs*

The FPs of system (1.2) can be determined by solving the subsequent nonlinear equations:

$$\begin{cases} x = \frac{x}{r(1+y)+\kappa x} - hx = f(x,y), \\ y = \sigma(1+x)y = g(x,y), \end{cases} \tag{2.1}$$

for $x$ and $y$. The system (1.2) possesses three FPs: $E_0 = (0,0)$, $E_1 = (\frac{1-r-hr}{\kappa+\kappa h}, 0)$, and

$$E_2 = \Big(\frac{1-\sigma}{\sigma}, \frac{1}{r}\Big(\kappa - \frac{\kappa}{\sigma} + \frac{1}{1+h} - r\Big)\Big).$$

$E_0 = (0,0)$ is the trivial FP that exists always. $E_1 = (\frac{1-r-hr}{\kappa+\kappa h}, 0)$ is a boundary FP that exists if $r + rh < 1$. Moreover, $E_2 = \Big(\frac{1-\sigma}{\sigma}, \frac{1}{r}\Big(\kappa - \frac{\kappa}{\sigma} + \frac{1}{1+h} - r\Big)\Big)$ is coexistence FP, which exists if $r < 1$, $\frac{\kappa}{1+\kappa-r} < \sigma < 1$, and $h < \frac{\sigma}{\kappa-\kappa\sigma+\sigma r} - 1$.

*2.2. Stability of FPs*

The Jacobian matrix of the system

$$\begin{cases} x_{n+1} = f(x_n, y_n) \\ y_{n+1} = g(x_n, y_n) \end{cases}$$

is the matrix given below:

$$J(x,y) = \begin{bmatrix} \frac{\partial f}{\partial x} & \frac{\partial f}{\partial y} \\ \frac{\partial g}{\partial x} & \frac{\partial g}{\partial y} \end{bmatrix}.$$

Thus, the Jacobian matrix $J(x,y)$ of the system (1.2) evaluated at any FP $(x,y)$ is as follows:

$$J(x,y) = \begin{bmatrix} \frac{r+ry-h(r+\kappa x+ry)^2}{(r+\kappa x+ry)^2} & -\frac{rx}{(r+\kappa x+ry)^2} \\ \sigma y & \sigma(1+x) \end{bmatrix}.$$

The eigenvalues $\xi_{1,2}$ of the Jacobian matrix $J$ are helpful in determining the stability of FPs. The FP $(x,y)$ is called a sink if $|\xi_{1,2}| < 1$ and a source if $|\xi_1| > 1$ and $|\xi_2| > 1$. Furthermore, the FP $(x,y)$ is classified as a saddle point (SP) if $|\xi_1| > 1$ and $|\xi_2| < 1$ (or $|\xi_1| < 1$ and $|\xi_2| > 1$). In the case of a non-hyperbolic point (NHBP) $(x,y)$, either $|\xi_1| = 1$ or $|\xi_2| = 1$. However, if the eigenvalues are in complicated form, making direct use of this definition challenging, the following result proves to be very useful in determining the stability of the FP.

**Lemma 2.1.** *[45] Let $\Lambda(\xi) = \xi^2 + K_1\xi + K_0$. Assume that $\Lambda(1) > 0$. If $\xi_1$ and $\xi_2$ are solutions of $\Lambda(\xi) = 0$, then*
*(1) $|\xi_1| < 1$ together with $|\xi_2| < 1$ if $\Lambda(-1) > 0 \wedge K_0 < 1$,*
*(2) $|\xi_1| < 1 \wedge |\xi_2| > 1$ (or $|\xi_1| > 1 \wedge |\xi_2| < 1$) if $\Lambda(-1) < 0$,*
*(3) $|\xi_{1,2}| > 1$ if $\Lambda(-1) > 0 \wedge K_0 > 1$,*
*(4) $|\xi_2| \neq 1 \wedge \xi_1 = -1$ if $\Lambda(-1) = 0 \wedge K_1 \neq 0, 2$,*
*(5) $\xi_1, \xi_2 \in \mathbb{C}$ along with $|\xi_{1,2}| = 1$ if $K_1^2 - 4K_0 < 0 \wedge K_0 = 1$.*

A sink reflects the long-term coexistence of herbivores and plants, suggesting a balanced environment in which populations maintain sustainable levels throughout time. An SP suggests intermittent stability, with the system alternating between plenty and shortage, similar to natural population fluctuations. An unstable source suggests vulnerability to unexpected changes, stressing the potential for population collapses or rapid expansion that disrupts ecological equilibrium. Furthermore, non-hyperbolic points may indicate intricate and nuanced interactions, demonstrating the complexity of ecological dynamics and the difficulty of predicting population behavior. Through computations, it is obtained that

$$J(E_0) = \begin{bmatrix} -h + \frac{1}{r} & 0 \\ 0 & \sigma \end{bmatrix}.$$

One can easily obtain the following result for the topological classification of $E_0$:

**Theorem 2.2.** *$E_0$ is a*
*(1) sink if $\sigma < 1$ and $\frac{1-r}{r} < h < \frac{1+r}{r}$,*
*(2) source if one of the below-listed parametric conditions is fulfilled:*
*(i) $\sigma > 1, r < 1,$ and $h < \frac{1-r}{r}$,*
*(ii) $\sigma > 1$ and $h > \frac{1+r}{r}$,*
*(3) SP if one of the listed below parametric conditions is fulfilled:*
*(i) $\sigma < 1, r < 1,$ and $h < \frac{1-r}{r}$,*
*(ii) $\sigma < 1$ and $h > \frac{1+r}{r}$,*
*(iii) $\sigma > 1$ and $\frac{1-r}{r} < h < \frac{1+r}{r}$,*
*(4) NHBP if one of the listed below parametric conditions is fulfilled:*
*(i) $\sigma = 1$ ,*
*(ii) $h = \frac{1+r}{r}$,*
*(iii) $r < 1$, $h = \frac{1-r}{r}$.*

The eigenvectors corresponding to eigenvalues $\xi_1 = -h + \frac{1}{r}$ and $\xi_2 = \sigma$ of $J(E_0)$ are $v_1 =< 1, 0 >$ and $v_2 =< 0, 1 >$. The stable $W^s$ and unstable $W^u$ manifolds in the saddle case (3-iii) are given by

$$W^s = \text{Span}(\{v_1\}),\ W^u = \text{Span}(\{v_2\}).$$

**Remark 2.3.** *At NHBP, the system experiences different types of bifurcations depending on the nature of the eigenvalues of the Jacobian matrix. If (4-i) is true, it follows that one of the eigenvalues of the matrix $J(E_0)$ is 1. Consequently, a TC bifurcation occurs at $E_0$. Similarly, a TC bifurcation occurs at $E_0$ if (4-iii) is true. Moreover, if (4-ii) is true, it follows that one of the eigenvalues of the matrix $J(E_0)$ is $-1$. Consequently, a PD bifurcation occurs at $E_0$.*

Next, we obtain

$$J(E_1) = \begin{bmatrix} r + h^2 r + h(-1 + 2r) & \frac{(1+h)r(-1+r+hr)}{\kappa} \\ 0 & \sigma - \frac{\sigma(-1+r+hr)}{\kappa(1+h)} \end{bmatrix}.$$

Since $E_1$ exists if $r < \frac{1}{1+h}$. Thus, we obtain the following result:

**Theorem 2.4.** *$E_1$ is a*

*(1) sink if $\frac{h-1}{(h+1)^2} < r < \frac{1}{h+1}$ and $0 < \sigma < \frac{\kappa+\kappa h}{\kappa+\kappa h-r-hr+1}$,*
*(2) source if $r < \frac{h-1}{(h+1)^2}, h > 1$ and $\sigma > \frac{\kappa+\kappa h}{\kappa+\kappa h-r-hr+1}$,*
*(3) SP if any of the following criteria is met:*
*(i) $r < \frac{h-1}{(h+1)^2}, h > 1$, and $0 < \sigma < \frac{\kappa+\kappa h}{\kappa+\kappa h-r-hr+1}$,*
*(ii) $\sigma > \frac{\kappa+\kappa h}{\kappa+\kappa h-r-hr+1}$ and $\frac{h-1}{(h+1)^2} < r < \frac{1}{h+1}$,*
*(4) NHBP if one of the listed below criteria is met:*
*(i) $r = \frac{h-1}{(h+1)^2}$,*
*(ii) $\sigma = \frac{\kappa+\kappa h}{\kappa+\kappa h-r-hr+1}$.*

The eigenvectors corresponding to eigenvalues $\xi_1 = r + h^2 r + h(-1 + 2r)$ and $\xi_2 = \sigma - \frac{\sigma(-1+r+hr)}{\kappa(1+h)}$ are $v_1 =< 1, 0 >$ and

$$v_2 = \langle 0, -\frac{r(1 + h)^2(-1 + r + rh)}{-\kappa h(1 + h) - \sigma(1 + \kappa + \kappa h) + \sigma r(1 + h) + \kappa r(1 + h)^3}\rangle.$$

The stable $W^s$ and unstable $W^u$ manifolds in the saddle case (3-ii) are given by

$$W^s = \text{Span}(\{v_1\}),\ W^u = \text{Span}(\{v_2\}).$$

**Remark 2.5.** *If (4-i) is true, then it follows that one of the eigenvalues of the matrix $J(E_1)$ is $-1$. Consequently, a PD bifurcation occurs at $E_1$. Moreover, if (4-ii) is true, it follows that one of the eigenvalues of the matrix $J(E_1)$ is 1. Consequently, a TC bifurcation occurs at $E_1$.*

The Jacobian matrix at positive FP is

$$J(E_2) = \begin{bmatrix} 1 + \frac{\kappa(-1+\sigma)(1+h)^2}{\sigma} & \frac{(-1+\sigma)(1+h)^2 r}{\sigma} \\ \frac{\sigma(\kappa - \frac{\kappa}{\sigma} + \frac{1}{1+h} - r)}{r} & 1 \end{bmatrix}. \tag{2.2}$$

The characteristic polynomial of $J(E_2)$ is

$$\Lambda(\xi) = \xi^2 + K_1\xi + K_0,$$

where

$$K_1 = -2 - \frac{\kappa(-1 + \sigma)(1 + h)^2}{\sigma},$$
$$K_0 = 2 - \sigma + h - \sigma h - \frac{\kappa(-2 + \sigma)(-1 + \sigma)(1 + h)^2}{\sigma} + (-1 + \sigma)(1 + h)^2 r.$$

Through computations, it is obtained that

$$\Lambda(0) = 2 - \sigma + h - \sigma h - \frac{\kappa(-2 + \sigma)(-1 + \sigma)(1 + h)^2}{\sigma} + (-1 + \sigma)(1 + h)^2 r,$$
$$\Lambda(-1) = 5 - \sigma + h - \sigma h - \frac{\kappa(-3 + \sigma)(-1 + \sigma)(1 + h)^2}{\sigma} + (-1 + \sigma)(1 + h)^2 r,$$

$$\Lambda(1) = \frac{(1-\sigma)(1+h)(\sigma + (1+h)(\kappa(-1+\sigma) - \sigma r))}{\sigma}.$$

After applying Lemma 2.1, we obtain the following result for the classification of the positive FP, $E_2$, of system (1.2).

**Theorem 2.6.** *The positive FP*

*(1) $E_2$ is a sink if $r < \frac{1}{\sigma(1+h)}(\sigma + \kappa\sigma + \kappa\sigma h - 2\kappa - 2h)$ and*

$$r > \frac{1}{(\sigma-1)(1+h)^2}\Big(-5 + \sigma - h + \sigma h + \frac{\kappa(\sigma-3)(\sigma-1)(1+h)^2}{\sigma}\Big),$$

*(2) $E_2$ is a source if $r > \frac{1}{\sigma(1+h)}(\sigma + \kappa\sigma + \kappa\sigma h - 2\kappa - 2h)$ and*

$$r > \frac{1}{(\sigma-1)(1+h)^2}\Big(-5 + \sigma - h + \sigma h + \frac{\kappa(\sigma-3)(\sigma-1)(1+h)^2}{\sigma}\Big),$$

*(3) $E_2$ is an SP if $r < \frac{1}{(\sigma-1)(1+h)^2}\Big(-5 + \sigma - h + \sigma h + \frac{\kappa(\sigma-3)(\sigma-1)(1+h)^2}{\sigma}\Big)$,*

*(4) $E_2$ is NHBP and experiences PD bifurcation if $\sigma \neq \frac{\kappa(1+h)^2}{2+\kappa(1+h)^2}, \frac{\kappa(1+h)^2}{4+\kappa(1+h)^2}$ and*

$$r = \frac{1}{(\sigma-1)(1+h)^2}\Big(-5 + \sigma - h + \sigma h + \frac{\kappa(\sigma-3)(\sigma-1)(1+h)^2}{\sigma}\Big),$$

*(5) $E_2$ is NHBP and experiences NS bifurcation if $0 < \kappa < \frac{4}{(1-\sigma)(1+h)^2}$ and*

$$r = \frac{1}{\sigma(1+h)}(\sigma + \kappa\sigma + \kappa\sigma h - 2\kappa - 2\kappa h).$$

## 3. Bifurcation analysis

This section aims to thoroughly investigate bifurcation phenomena, including TC bifurcation at $E_1$ as well as PD and NS bifurcations at $E_2$. For a comprehensive understanding of bifurcation analysis, we suggest referring to the sources [46–49]. Bifurcation is a crucial factor in determining the dynamics of the system, revealing situations where even little changes in parameters may lead to significant changes in plant-herbivore interactions. Moreover, exploring bifurcation processes improves our comprehension of ecosystem dynamics, facilitating the development of effective strategies for preserving and controlling plant and herbivore populations in a sustainable manner.

### *3.1. TC bifurcation at $E_1$*

We start our examination of the TC bifurcation at $E_1$ by considering condition (4-ii) outlined in Theorem 2.4. We can rewrite it as $r = \frac{-\kappa - h\kappa + \sigma + \kappa\sigma + h\kappa\sigma}{(1+h)\sigma}$. Introducing a sufficiently small perturbation $\varepsilon$ into the bifurcation parameter $r$ around $R_{10} = \frac{-\kappa - h\kappa + \sigma + \kappa\sigma + h\kappa\sigma}{(1+h)\sigma}$, the system (1.2) takes the subsequent form:

$$\begin{cases} x_{n+1} = \frac{x_n}{(R_{10}+\varepsilon)(1+y_n)+\kappa x_n} - hx_n, \\ y_{n+1} = \sigma(1+x_n)y_n. \end{cases} \tag{3.1}$$

We shift $E_1$ to $(0,0)$ by taking $u_n = x_n - \frac{1-(R_{10}+\varepsilon)-h(R_{10}+\varepsilon)}{\kappa+\kappa h}$, $v_n = y_n$. Consequently, the system (3.1) becomes

$$\begin{bmatrix} u_{n+1} \\ v_{n+1} \end{bmatrix} = \begin{bmatrix} 1+\frac{(1+h)^2\kappa(-1+\sigma)}{\sigma} & \frac{(1+h)(-1+\sigma)((1+h)\kappa(-1+\sigma)+\sigma)}{\sigma^2} \\ 0 & 1 \end{bmatrix} \begin{bmatrix} u_n \\ v_n \end{bmatrix} + \begin{bmatrix} F(u_n, v_n, \varepsilon) \\ G(u_n, v_n, \varepsilon) \end{bmatrix}, \tag{3.2}$$

where

$$\begin{aligned}
F(u_n, v_n, \varepsilon) &= a_1 u_n^2 + a_2 v_n^2 + a_3 u_n v_n + a_4 u_n \varepsilon + a_5 v_n \varepsilon + a_6 u_n^3 + a_7 v_n^3 + a_8 u_n^2 v_n + a_9 u_n^2 \varepsilon \\
&\quad + a_{10} u_n v_n^2 + a_{11} v_n^2 \varepsilon + a_{12} v_n \varepsilon^2 + a_{13} u_n v_n \varepsilon + O((|u_n| + |v_n| + |\varepsilon|)^4), \\
G(u_n, v_n, \varepsilon) &= b_1 u_n v_n + b_2 v_n \varepsilon + O((|u_n| + |v_n| + |\varepsilon|)^4), \\
a_1 &= -\frac{(1+h)^2\kappa((1+h)\kappa(-1+\sigma)+\sigma)}{\sigma},\ a_2 = -\frac{(1+h)(-1+\sigma)((1+h)\kappa(-1+\sigma)+\sigma)^2}{\sigma^3}, \\
a_3 &= -\frac{(1+h)((1+h)\kappa(-1+\sigma)+\sigma)(2(1+h)\kappa(-1+\sigma)+\sigma)}{\sigma^2},\ a_4 = (1+h)^2, \\
a_5 &= \frac{(1+h)(2(1+h)\kappa(-1+\sigma)+\sigma)}{\kappa\sigma},\ a_6 = \frac{(1+h)^3\kappa^2((1+h)\kappa(-1+\sigma)+\sigma)}{\sigma}, \\
a_7 &= \frac{(1+h)(-1+\sigma)((1+h)\kappa(-1+\sigma)+\sigma)^3}{\sigma^4}, \\
a_8 &= \frac{(1+h)^2\kappa((1+h)\kappa(-1+\sigma)+\sigma)(3(1+h)\kappa(-1+\sigma)+2\sigma)}{\sigma^2},\ a_9 = -(1+h)^3\kappa, \\
a_{10} &= \frac{(1+h)((1+h)\kappa(-1+\sigma)+\sigma)^2(3(1+h)\kappa(-1+\sigma)+\sigma)}{\sigma^3}, \\
a_{11} &= -\frac{(1+h)((1+h)\kappa(-1+\sigma)+\sigma)(3(1+h)\kappa(-1+\sigma)+\sigma)}{\kappa\sigma^2},\ a_{12} = \frac{(1+h)^2}{\kappa}, \\
a_{13} &= -\frac{(1+h)^2(4(1+h)\kappa(-1+\sigma)+3\sigma)}{\sigma},\ b_1 = \sigma,\ b_2 = -\frac{\sigma}{\kappa}.
\end{aligned}$$

Next, the system (3.2) is diagonalized through the consideration of the following transformation:

$$\begin{bmatrix} u_n \\ v_n \end{bmatrix} = \begin{bmatrix} -1-\frac{1}{\kappa+h\kappa}+\frac{1}{\sigma} & 1 \\ 1 & 0 \end{bmatrix} \begin{bmatrix} e_n \\ f_n \end{bmatrix}, \tag{3.3}$$

Upon applying the mapping (3.3), the system (3.2) undergoes the alteration as follows:

$$\begin{bmatrix} e_{n+1} \\ f_{n+1} \end{bmatrix} = \begin{bmatrix} 1 & 0 \\ 0 & \xi \end{bmatrix} \begin{bmatrix} e_n \\ f_n \end{bmatrix} + \begin{bmatrix} \Gamma(e_n, f_n, \varepsilon) \\ \Upsilon(e_n, f_n, \varepsilon) \end{bmatrix}, \tag{3.4}$$

where

$$\xi = 1 + \frac{(1+h)^2\kappa(-1+\sigma)}{\sigma},$$

$$\Gamma(e_n, f_n, \varepsilon) = c_1 e_n^2 + c_2 e_n f_n + c_3 e_n \varepsilon + O((|e_n| + |f_n| + |\varepsilon|)^4),$$

$$\Upsilon(e_n, f_n, \varepsilon) = d_1 e_n^2 + d_2 f_n^2 + d_3 e_n f_n + d_4 e_n \varepsilon + d_5 f_n \varepsilon + d_6 f_n^3 + d_7 e_n^2 \varepsilon + d_8 e_n f_n^2 + d_9 f_n^2 \varepsilon + d_{10} e_n \varepsilon^2 + d_{11} e_n f_n \varepsilon + O((|e_n| + |f_n| + |\varepsilon|)^4),$$

$$c_1 = 1 - (1 + \frac{1}{\kappa + h\kappa})\sigma,\ c_2 = \sigma,\ c_3 = -\frac{\sigma}{\kappa},\ d_1 = -\frac{((1+h)\kappa(-1+\sigma)+\sigma)^2}{(1+h)^2\kappa^2\sigma},$$

$$d_2 = -\frac{(1+h)^2\kappa((1+h)\kappa(-1+\sigma)+\sigma)}{\sigma},\ d_3 = h + \frac{(1+h)^2\kappa(-1+\sigma)}{\sigma} + \sigma + \frac{\sigma}{\kappa + h\kappa},$$

$$d_4 = \frac{1-\sigma}{\kappa} + \frac{(1+h)^2(-1+\sigma)}{\sigma} - \frac{\sigma}{(1+h)\kappa^2},\ d_5 = (1+h)^2,$$

$$d_6 = \frac{(1+h)^3\kappa^2((1+h)\kappa(-1+\sigma)+\sigma)}{\sigma},\ d_7 = \frac{(1+h)((1+h)\kappa(-1+\sigma)+\sigma)}{\kappa\sigma},$$

$$d_8 = -\frac{(1+h)^2\kappa((1+h)\kappa(-1+\sigma)+\sigma)}{\sigma},\ d_9 = -(1+h)^3\kappa,$$

$$d_{10} = \frac{(1+h)^2}{\kappa},\ d_{11} = -\frac{(1+h)^2(2(1+h)\kappa(-1+\sigma)+\sigma)}{\sigma}.$$

Now, we use the center manifold theory to obtain the center manifold $M^C$ of (3.2) at $(0,0)$ in a close neighborhood of $\varepsilon = 0$. The center manifold $M^C$ can be obtained using

$$M^C = \left\{(e_n, f_n, \varepsilon) \in \mathbb{R}^3_+ \middle| f_n = p_1 e_n^2 + p_2 e_n \varepsilon + p_3 \varepsilon^2 + O(3)\right\}.$$

Through calculations, we obtain $p_1 = \frac{d_1}{1-\xi}, p_2 = \frac{d_4}{1-\xi}, p_3 = 0$. Consequently, the system (3.2) is restricted to $M^C$ as follows:

$$\omega := e_{n+1} = e_n + c_1 e_n^2 + c_3 e_n \varepsilon + (\frac{c_2 d_1}{1-\xi}) e_n^3 + (\frac{c_2 d_4}{1-\xi}) e_n^2 \varepsilon + O(4). \tag{3.5}$$

Through simple computations, we obtain

$$\omega(0,0) = 0,\ \omega_{e_n}(0,0) = 1,\ \omega_{\varepsilon}(0,0) = 0,$$
$$\omega_{e_n e_n}(0,0) = 2c_1 = 2 - 2(1 + \frac{1}{\kappa + h\kappa})\sigma \neq 0,$$
$$\omega_{e_n \varepsilon}(0,0) = c_3 = -\frac{\sigma}{\kappa} \neq 0.$$

Thus, the system (1.2) experiences TC bifurcation at $E_1$. The next result gives the conditions for the existence and direction of TC bifurcation in the system (1.2) at $E_1$.

**Theorem 3.1.** *If condition (4-ii) in Theorem 2.4 is fulfilled, then* (1.2) *undergoes TC bifurcation at* $E_1$ *when* $r$ *differs in a close neighborhood of* $R_{10} = \frac{-\kappa - h\kappa + \sigma + \kappa\sigma + h\kappa\sigma}{(1+h)\sigma}$.

The boundary FP is unstable for $r < R_{10}$. It collides with positive FP at $r = R_{10}$, and subsequently they exchange stability. The result shows that small variations in environmental or biological parameters may cause major modifications in plant-herbivore population dynamics, culminating in a TC bifurcation at the border fixed point. At the transition, essential ecosystem dynamics shift, causing the system to shift from a state of stable coexistence between plants and herbivores to one in which plants can live on their own.

### 3.2. PD bifurcation at $E_2$

Next, we investigate the PD bifurcation at $E_2$ by considering condition (4) presented in Theorem 2.6. Biologically, PD bifurcations indicate significant alterations in plant-herbivore dynamics. Consider a situation in which plant and herbivore populations vary regularly over time. During a PD bifurcation, these variations become more intense, and the space between peak and trough densities widens, perhaps doubling. This may have a severe environmental effect. If environmental circumstances unexpectedly favor plant growth, herbivore populations may increase, thereby depleting plant resources. Plant populations rebound when herbivore numbers drop. However, when plant numbers recover, herbivore populations rebound, resulting in increased grazing pressure and a consequent drop in plant populations. Introducing a sufficiently small perturbation $\varepsilon$ into the bifurcation parameter $r$ around $R_1 = \frac{1}{(\sigma-1)(1+h)^2}\Big(-5+\sigma-h+\sigma h+\frac{\kappa(\sigma-3)(\sigma-1)(1+h)^2}{\sigma}\Big)$, the system (1.2) takes the subsequent form:

$$\begin{cases} x_{n+1} = \frac{x_n}{(R_1+\varepsilon)(1+y_n)+\kappa x_n} - hx_n, \\ y_{n+1} = \sigma(1+x_n)y_n. \end{cases} \tag{3.6}$$

To translate the point $E_2$ at $(0,0)$, we use the change of variables $u_n = x_n - \frac{1-\sigma}{\sigma},\ v_n = y_n - \frac{1}{(R_1+\varepsilon)}\Big(\kappa - \frac{\kappa}{\sigma} + \frac{1}{1+h} - (R_1+\varepsilon)\Big)$. Consequently, the system (3.6) is expressed as below:

$$\begin{bmatrix} u_{n+1} \\ v_{n+1} \end{bmatrix} = \begin{bmatrix} 1+\frac{\kappa(-1+\sigma)(1+h)^2}{\sigma} & \frac{\kappa(3-4\sigma+\sigma^2)(1+h)^2+\sigma(-5+\sigma-h+\sigma h)}{\sigma^2} \\ \frac{2\sigma(2\sigma+\kappa(-1+\sigma)(1+h)^2)}{\kappa(3-4\sigma+\sigma^2)(1+h)^2+\sigma(-5+\sigma-h+\sigma h)} & 1 \end{bmatrix} \begin{bmatrix} u_n \\ v_n \end{bmatrix} + \begin{bmatrix} \Pi_1(u_n,v_n,\varepsilon) \\ \Pi_2(u_n,v_n,\varepsilon) \end{bmatrix}, \tag{3.7}$$

where

$$\begin{aligned}
\Pi_1(u_n,v_n,\varepsilon) &= a_1u_n^2 + a_2v_n^2 + a_3u_nv_n + a_4v_n\varepsilon + a_5u_n^3 + a_6v_n^3 + a_7u_n^2v_n + a_8u_nv_n^2 + a_9v_n^2\varepsilon + a_{10}u_nv_n\varepsilon + O(4), \\
\Pi_2(u_n,v_n,\varepsilon) &= b_1u_nv_n + b_2u_n\varepsilon + b_3u_n\varepsilon^2 + O(4), \\
a_1 &= -\frac{\kappa(1+h)^2(\sigma+\kappa(-1+\sigma)(1+h))}{\sigma},\ a_2 = -\frac{(\kappa(3-4\sigma+\sigma^2)(1+h)^2+\sigma(-5+\sigma-h+\sigma h))^2}{(-1+\sigma)\sigma^3(1+h)}, \\
a_3 &= -\frac{(\sigma+2\kappa(-1+\sigma)(1+h))(\kappa(3-4\sigma+\sigma^2)(1+h)^2+\sigma(-5+\sigma-h+\sigma h))}{(-1+\sigma)\sigma^2}, \\
a_4 &= \frac{(-1+\sigma)(1+h)^2}{\sigma},\ a_5 = \frac{\kappa^2(1+h)^3(\sigma+\kappa(-1+\sigma)(1+h))}{\sigma}, \\
a_6 &= \frac{(\kappa(3-4\sigma+\sigma^2)(1+h)^2+\sigma(-5+\sigma-h+\sigma h))^3}{(-1+\sigma)^2\sigma^4(1+h)^2}, \\
a_7 &= \frac{\kappa(1+h)(2\sigma+3\kappa(-1+\sigma)(1+h))(\kappa(3-4\sigma+\sigma^2)(1+h)^2+\sigma(-5+\sigma-h+\sigma h))}{(-1+\sigma)\sigma^2}, \\
a_8 &= \frac{(\sigma+3\kappa(-1+\sigma)(1+h))(\kappa(3-4\sigma+\sigma^2)(1+h)^2+\sigma(-5+\sigma-h+\sigma h))^2}{(-1+\sigma)^2\sigma^3(1+h)}, \\
a_9 &= -\frac{2(1+h)(\kappa(3-4\sigma+\sigma^2)(1+h)^2+\sigma(-5+\sigma-h+\sigma h))}{\sigma^2}, \\
a_{10} &= -\frac{(1+h)^2(\sigma+2\kappa(-1+\sigma)(1+h))}{\sigma},
\end{aligned}$$

$$b_1 = \sigma,\ b_2 = -\frac{(-1+\sigma)^2\sigma^2(1+h)^3(\sigma+\kappa(-1+\sigma)(1+h))}{(\kappa(3-4\sigma+\sigma^2)(1+h)^2+\sigma(-5+\sigma-h+\sigma h))^2},$$
$$b_3 = \frac{(-1+\sigma)^3\sigma^3(1+h)^5(\sigma+\kappa(-1+\sigma)(1+h))}{(\kappa(3-4\sigma+\sigma^2)(1+h)^2+\sigma(-5+\sigma-h+\sigma h))^3}.$$

Subsequently, the system (3.7) goes through diagonalization after a consideration of the following transformation:

$$\begin{bmatrix} u_n \\ v_n \end{bmatrix} = \begin{bmatrix} \frac{-\kappa(3-4\sigma+\sigma^2)(1+h)^2+\sigma(5+h-\sigma(1+h))}{\sigma(2\sigma+\kappa(-1+\sigma)(1+h)^2)} & \frac{\kappa(3-4\sigma+\sigma^2)(1+h)^2+\sigma(-5+\sigma-h+\sigma h)}{2\sigma^2} \\ 1 & 1 \end{bmatrix} \begin{bmatrix} e_n \\ f_n \end{bmatrix}. \tag{3.8}$$

After implementing the map (3.8), the system (3.7) takes the subsequent form:

$$\begin{bmatrix} e_{n+1} \\ f_{n+1} \end{bmatrix} = \begin{bmatrix} -1 & 0 \\ 0 & \xi \end{bmatrix} \begin{bmatrix} e_n \\ f_n \end{bmatrix} + \begin{bmatrix} \Gamma(e_n, f_n, \varepsilon) \\ \Upsilon(e_n, f_n, \varepsilon) \end{bmatrix}, \tag{3.9}$$

where

$$\xi = 3 + \frac{\kappa(-1+\sigma)(1+h)^2}{\sigma},$$

$$\begin{aligned}
\Gamma(e_n, f_n, \varepsilon) &= c_1e_n^2 + c_2f_n^2 + c_3e_nf_n + c_4e_n\varepsilon + c_5f_n\varepsilon + c_6e_n^3 + c_7f_n^3 + c_8e_n^2f_n \\
&\quad + c_9e_n^2\varepsilon + c_{10}e_nf_n^2 + c_{11}f_n^2\varepsilon + c_{12}e_n\varepsilon^2 + c_{13}f_n\varepsilon^2 + c_{14}e_nf_n\varepsilon + O(4), \\
\Upsilon(e_n, f_n, \varepsilon) &= d_1e_n^2 + d_2f_n^2 + d_3e_nf_n + d_4e_n\varepsilon + d_5f_n\varepsilon + d_6e_n^3 + d_7f_n^3 + d_8e_n^2f_n \\
&\quad + d_9e_n^2\varepsilon + d_{10}e_nf_n^2 + d_{11}f_n^2\varepsilon + d_{12}e_n\varepsilon^2 + d_{13}f_n\varepsilon^2 + d_{14}e_nf_n\varepsilon + O(4), \\
c_1 &= -\frac{(\kappa(3-4\sigma+\sigma^2)(1+h)^2+\sigma(\sigma-5-h+\sigma h))(\kappa(\sigma-1)^2(1+h)^3+2\sigma(\sigma-3+h+\sigma h))}{(-1+\sigma)(1+h)(2\sigma+\kappa(-1+\sigma)(1+h)^2)(4\sigma+\kappa(-1+\sigma)(1+h)^2)},
\end{aligned}$$

$$\begin{aligned}
c_2 &= ((2\sigma+\kappa(-1+\sigma)(1+h)^2)(\kappa(3-4\sigma+\sigma^2)(1+h)^2+\sigma(-5+\sigma-h \\
&\quad +\sigma h))(\kappa^2(-1+\sigma)^2(1+h)^4+\kappa(-1+\sigma)\sigma(1+h)^2(5+h)+\sigma^2(5+\sigma \\
&\quad +h+\sigma h)))/(2(-1+\sigma)\sigma^3(1+h)(4\sigma+\kappa(-1+\sigma)(1+h)^2)), \\
c_3 &= \frac{(16\sigma+\kappa(\sigma-1)(1+h)^2(5+\sigma-3h+\sigma h))(\kappa(3-4\sigma+\sigma^2)(1+h)^2+\sigma(\sigma-5-h+\sigma h))}{2(\sigma-1)\sigma(1+h)(4\sigma+\kappa(\sigma-1)(1+h)^2)}, \\
c_4 &= \frac{(-1+\sigma)\sigma(1+h)^2}{4\sigma+\kappa(-1+\sigma)(1+h)^2}, \\
c_5 &= -\frac{(\sigma-1)(1+h)^2(2\sigma+\kappa(\sigma-1)(1+h)^2)(\kappa(\sigma-1)^2(1+h)^2+\sigma(3+\sigma-h+\sigma h))}{2(4\sigma+\kappa(-1+\sigma)(1+h)^2)(\kappa(3-4\sigma+\sigma^2)(1+h)^2+\sigma(-5+\sigma-h+\sigma h))}, \\
c_6 &= \frac{8\sigma(-1+h)(\kappa(3-4\sigma+\sigma^2)(1+h)^2+\sigma(-5+\sigma-h+\sigma h))^2}{(-1+\sigma)^2(1+h)^2(2\sigma+\kappa(-1+\sigma)(1+h)^2)^2(4\sigma+\kappa(-1+\sigma)(1+h)^2)}, \\
c_7 &= -(((2\sigma+\kappa(\sigma-1)(1+h)^2)^3(\kappa(\sigma-1)(1+h)^2+\sigma(3+h))(\kappa(3-4\sigma+\sigma^2)(1+h)^2 \\
&\quad +\sigma(-5+\sigma-h+\sigma h))^2)/(4(\sigma-1)^2\sigma^5(1+h)^2(4\sigma+\kappa(\sigma-1)(1+h)^2))),
\end{aligned}$$

$$c_8 = \frac{4(\sigma(h-5)+\kappa(\sigma-1)(h-2)(1+h)^2)(\kappa(3-4\sigma+\sigma^2)(1+h)^2+\sigma(\sigma-5-h+\sigma h))^2}{(\sigma-1)^2\sigma(1+h)^2(2\sigma+\kappa(\sigma-1)(1+h)^2)(4\sigma+\kappa(\sigma-1)(1+h)^2)},$$

$$c_9 = -\frac{2\sigma(-3+h)(1+h)}{4\sigma+\kappa(-1+\sigma)(1+h)^2},$$

$$c_{10} = ((2\sigma+\kappa(-1+\sigma)(1+h)^2)(\kappa(-1+\sigma)(-5+h)(1+h)^2-2\sigma(7+h))(\kappa(3-4\sigma$$
$$+\sigma^2)(1+h)^2+\sigma(-5+\sigma-h+\sigma h))^2)/(2(-1+\sigma)^2\sigma^3(1+h)^2(4\sigma+\kappa(-1+\sigma)(1+h)^2)),$$

$$c_{11} = \frac{(1+h)(2\sigma+\kappa(-1+\sigma)(1+h)^2)(2\kappa(-1+\sigma)(1+h)^2+\sigma(5+h))}{\sigma(4\sigma+\kappa(-1+\sigma)(1+h)^2)},$$

$$c_{12} = -\frac{(-1+\sigma)^3\sigma^2(1+h)^5(\sigma+\kappa(-1+\sigma)(1+h))}{(4\sigma+\kappa(-1+\sigma)(1+h)^2)(\kappa(3-4\sigma+\sigma^2)(1+h)^2+\sigma(-5+\sigma-h+\sigma h))^2},$$

$$c_{13} = \frac{(-1+\sigma)^3\sigma(1+h)^5(\sigma+\kappa(-1+\sigma)(1+h))(2\sigma+\kappa(-1+\sigma)(1+h)^2)}{2(4\sigma+\kappa(-1+\sigma)(1+h)^2)(\kappa(3-4\sigma+\sigma^2)(1+h)^2+\sigma(-5+\sigma-h+\sigma h))^2},$$

$$c_{14} = \frac{(1+h)(16\sigma^2+2\kappa^2(-1+\sigma)^2(1+h)^4+\kappa(-1+\sigma)\sigma(1+h)^2(9+h))}{\sigma(4\sigma+\kappa(-1+\sigma)(1+h)^2)},$$

$$d_1 = -\frac{2\sigma(1+\sigma-3h+\sigma h)(\kappa(3-4\sigma+\sigma^2)(1+h)^2+\sigma(-5+\sigma-h+\sigma h))}{(-1+\sigma)(1+h)(2\sigma+\kappa(-1+\sigma)(1+h)^2)(4\sigma+\kappa(-1+\sigma)(1+h)^2)},$$

$$d_2 = -(((\kappa^3(-1+\sigma)^3(1+h)^6+4\kappa(-1+\sigma)\sigma^2(1+h)^2(4+h)+\kappa^2(-1+\sigma)^2\sigma(1+h)^4(7$$
$$+h)-2\sigma^3(-7+\sigma-3h+\sigma h))(\kappa(3-4\sigma+\sigma^2)(1+h)^2+\sigma(-5+\sigma-h+\sigma h)))/(2(-1$$
$$+\sigma)\sigma^3(1+h)(4\sigma+\kappa(-1+\sigma)(1+h)^2))),$$

$$d_3 = ((\kappa(3-4\sigma+\sigma^2)(1+h)^2+\sigma(-5+\sigma-h+\sigma h))(-16\sigma^2+\kappa^2(-1+\sigma)^2(-3$$
$$+h)(1+h)^4+\kappa(-1+\sigma)\sigma(1+h)^2(-15+\sigma+h+\sigma h)))/((-1+\sigma)\sigma(1+h)(2\sigma$$
$$+\kappa(-1+\sigma)(1+h)^2)(4\sigma+\kappa(-1+\sigma)(1+h)^2)),$$

$$d_4 = \frac{2(\sigma-1)\sigma(1+h)^2(\kappa\sigma(2\sigma-3+\sigma^2)(1+h)^2+\kappa^2(\sigma-1)^2(1+h)^4+\sigma^2(3+\sigma-h+\sigma h))}{(2\sigma+\kappa(\sigma-1)(1+h)^2)(4\sigma+\kappa(\sigma-1)(1+h)^2)(\kappa(3-4\sigma+\sigma^2)(1+h)^2+\sigma(\sigma-5-h+\sigma h))},$$

$$d_5 = -\frac{(-1+\sigma)\sigma(1+h)^2}{4\sigma+\kappa(-1+\sigma)(1+h)^2},$$

$$d_6 = -\frac{8\sigma(-1+h)(\kappa(3-4\sigma+\sigma^2)(1+h)^2+\sigma(-5+\sigma-h+\sigma h))^2}{(-1+\sigma)^2(1+h)^2(2\sigma+\kappa(-1+\sigma)(1+h)^2)^2(4\sigma+\kappa(-1+\sigma)(1+h)^2)},$$

$$d_7 = ((2\sigma+\kappa(-1+\sigma)(1+h)^2)^3(\kappa(-1+\sigma)(1+h)^2+\sigma(3+h))(\kappa(3-4\sigma+\sigma^2)(1+h)^2$$
$$+\sigma(-5+\sigma-h+\sigma h))^2)/(4(-1+\sigma)^2\sigma^5(1+h)^2(4\sigma+\kappa(-1+\sigma)(1+h)^2)),$$

$$d_8 = -\frac{4(\sigma(h-5)+\kappa(\sigma-1)(h-2)(1+h)^2)(\kappa(3-4\sigma+\sigma^2)(1+h)^2+\sigma(\sigma-5-h+\sigma h))^2}{(-1+\sigma)^2\sigma(1+h)^2(2\sigma+\kappa(-1+\sigma)(1+h)^2)(4\sigma+\kappa(-1+\sigma)(1+h)^2)},$$

$$d_9 = \frac{2\sigma(-3+h)(1+h)}{4\sigma+\kappa(-1+\sigma)(1+h)^2},$$

$$d_{10} = -(((2\sigma+\kappa(-1+\sigma)(1+h)^2)(\kappa(-1+\sigma)(-5+h)(1+h)^2-2\sigma(7+h))(\kappa(3$$
$$-4\sigma+\sigma^2)(1+h)^2+\sigma(-5+\sigma-h+\sigma h))^2)/(2(-1+\sigma)^2\sigma^3(1+h)^2(4\sigma+\kappa(\sigma-1)(1+h)^2))),$$

$$d_{11} = -\frac{(1+h)(2\sigma+\kappa(-1+\sigma)(1+h)^2)(2\kappa(-1+\sigma)(1+h)^2+\sigma(5+h))}{\sigma(4\sigma+\kappa(-1+\sigma)(1+h)^2)},$$

$$d_{12} = -\frac{2(-1+\sigma)^3\sigma^3(1+h)^5(\sigma+\kappa(-1+\sigma)(1+h))}{(2\sigma+\kappa(\sigma-1)(1+h)^2)(4\sigma+\kappa(\sigma-1)(1+h)^2)(\kappa(3-4\sigma+\sigma^2)(1+h)^2+\sigma(\sigma-5-h+\sigma h))^2},$$

$$d_{13} = \frac{(-1+\sigma)^3\sigma^2(1+h)^5(\sigma+\kappa(-1+\sigma)(1+h))}{(4\sigma+\kappa(-1+\sigma)(1+h)^2)(\kappa(3-4\sigma+\sigma^2)(1+h)^2+\sigma(-5+\sigma-h+\sigma h))^2},$$

$$d_{14} = -\frac{(1+h)(16\sigma^2 + 2\kappa^2(-1+\sigma)^2(1+h)^4 + \kappa(-1+\sigma)\sigma(1+h)^2(9+h))}{\sigma(4\sigma + \kappa(-1+\sigma)(1+h)^2)}.$$

Now, we use the center manifold theory to obtain the center manifold $M^C$ of (3.9) at $(0,0)$ in a close neighborhood of $\varepsilon = 0$. Its approximation is as follows:

$$M^C = \left\{(e_n, f_n, \varepsilon) \in \mathbb{R}^3_+ \middle| f_n = p_1 e_n^2 + p_2 e_n \varepsilon + p_3 \varepsilon^2 + O(3)\right\},$$

where

$$p_1 = \frac{d_1}{1-\xi},\ p_2 = -\frac{d_4}{1+\xi},\ p_3 = 0.$$

Consequently, the system (3.9) is restricted to $M^C$ as follows:

$$\omega := e_{n+1} = -e_n + c_1 e_n^2 + c_4 e_n \varepsilon + \left(c_6 + \frac{c_3 d_1}{1-\xi}\right)e_n^3 + \left(c_9 + \frac{c_5 d_1}{1-\xi} - \frac{c_3 d_4}{1+\xi}\right)e_n^2 \varepsilon + \left(c_{12} - \frac{c_5 d_4}{1+\xi}\right)e_n \varepsilon^2 + O(4). \tag{3.10}$$

The mapping (3.10) undergoes PD bifurcation if the following are nonzero:

$$l_1 = \omega_\varepsilon \omega_{e_n e_n} + 2\omega_{e_n \varepsilon}\Big|_{(0,0)} = 2c_4, \tag{3.11}$$

$$l_2 = \frac{1}{2}(\omega_{e_n e_n})^2 + \frac{1}{3}\omega_{e_n e_n e_n}\Big|_{(0,0)} = 2\left(c_1^2 + c_6 + \frac{c_3 d_1}{1-\xi}\right). \tag{3.12}$$

Thus, we obtain the following result:

**Theorem 3.2.** *If condition (4) of Theorem 2.6 is fulfilled, then* (1.2) *undergoes PD bifurcation at* $E_2$ *if* $l_1, l_2$ *provided in* (3.11) *and* (3.12) *are nonzero and* $r$ *fluctuates in a small neighborhood of*

$$R_1 = \frac{1}{(\sigma-1)(1+h)^2}\left(-5 + \sigma - h + \sigma h + \frac{\kappa(\sigma-3)(\sigma-1)(1+h)^2}{\sigma}\right).$$

*Moreover, if* $l_2 > 0$ *(respectively,* $l_2 < 0$*), then an orbit of period-2 emanates from* $E_2$*, which is stable (respectively, unstable).*

The result illustrates how minor fluctuations in parameters can lead to substantial shifts in the system's dynamics, specifically causing a doubling of the population oscillation periods. This happens when the herbivore population increases and feeds more on the plants, thus leading to a reduction in the plant population. With fewer plants available, the herbivore population begins to decrease due to the lack of food. When the herbivore numbers decrease, the plant population is given the chance to increase once again, and the cycle begins again. This cycle reflects the delicate balance and complex interactions that exist within the environment.

### 3.3. NS bifurcation at $E_2$

Next, we investigate NS bifurcation at $E_2$ by considering condition (5) presented in Theorem 3.3. Biologically, NS bifurcations reveal complex dynamics within a plant-herbivore system, often marked by unexpected changes and unpredictable patterns. Imagine a situation in which the changes in the populations of plants and herbivores cannot be accurately predicted. NS bifurcation may cause population numbers to fluctuate significantly due to even minor alterations in environmental circumstances or plant-herbivore interactions, making it difficult to predict these changes. The instability has a dramatic effect on the dynamics of ecosystems, which presents issues for ecologists attempting to forecast how populations will respond to changes in the environment. For example, sudden changes in the environment may cause unpredictable and disorderly variations in populations of plants and herbivores, leading to disruptions in the interactions between different trophic levels and unpredictable changes in how the ecosystem functions. Introducing a sufficiently small perturbation $\varepsilon$ into the bifurcation parameter $r$ around $R_2 = \frac{1}{\sigma(1+h)}(\sigma + \kappa\sigma + \kappa\sigma h - 2\kappa - 2\kappa h)$, the system (1.2) takes the subsequent form:

$$\begin{cases} x_{n+1} = \frac{x_n}{(R_2+\varepsilon)(1+y_n)+\kappa x_n} - hx_n, \\ y_{n+1} = \sigma(1 + x_n)y_n. \end{cases} \tag{3.13}$$

We use the translation $u_n = x_n - \frac{1-\sigma}{\sigma}$, $v_n = y_n - \frac{1}{(R_2+\varepsilon)}\Big(\kappa - \frac{\kappa}{\sigma} + \frac{1}{1+h} - (R_2 + \varepsilon)\Big)$ to translate the point $E_2$ to origin. Consequently, the system (3.13) becomes

$$\begin{bmatrix} u_{n+1} \\ v_{n+1} \end{bmatrix} = \begin{bmatrix} 1 + \frac{\kappa(-1+\sigma)(1+h)^2}{\sigma} & \frac{(-1+\sigma)(1+h)(\kappa(-2+\sigma)(1+h)+\sigma(1+\varepsilon+h\varepsilon))}{\sigma^2} \\ \frac{\sigma(\frac{\kappa}{\sigma}-\varepsilon)}{\kappa-\frac{2\kappa}{\sigma}+\frac{1}{1+h}+\varepsilon} & 1 \end{bmatrix} \begin{bmatrix} u_n \\ v_n \end{bmatrix} + \begin{bmatrix} \Pi_1(u_n, v_n) \\ \Pi_2(u_n, v_n) \end{bmatrix}, \tag{3.14}$$

where

$$\begin{aligned}
\Pi_1(u_n, v_n) &= a_1u_n^2 + a_2v_n^2 + a_3u_nv_n + a_4u_n^3 + a_5v_n^3 + a_6u_n^2v_n + a_7u_nv_n^2 + O(4), \\
\Pi_2(u_n, v_n) &= \sigma u_nv_n, \\
a_1 &= -\frac{\kappa(1 + h)^2(\sigma + \kappa(-1 + \sigma)(1 + h))}{\sigma}, \; a_2 = -\frac{(-1 + \sigma)(1 + h)(\kappa(-2 + \sigma)(1 + h) + \sigma(1 + \varepsilon + h\varepsilon))^2}{\sigma^3}, \\
a_3 &= -\frac{(1 + h)(\sigma + 2\kappa(-1 + \sigma)(1 + h))(\kappa(-2 + \sigma)(1 + h) + \sigma(1 + \varepsilon + h\varepsilon))}{\sigma^2}, \\
a_4 &= \frac{\kappa^2(1 + h)^3(\sigma + \kappa(-1 + \sigma)(1 + h))}{\sigma}, \; a_5 = \frac{(-1 + \sigma)(1 + h)(\kappa(-2 + \sigma)(1 + h) + \sigma(1 + \varepsilon + h\varepsilon))^3}{\sigma^4}, \\
a_6 &= \frac{\kappa(1 + h)^2(2\sigma + 3\kappa(-1 + \sigma)(1 + h))(\kappa(-2 + \sigma)(1 + h) + \sigma(1 + \varepsilon + h\varepsilon))}{\sigma^2}, \\
a_7 &= \frac{(1 + h)(\sigma + 3\kappa(-1 + \sigma)(1 + h))(\kappa(-2 + \sigma)(1 + h) + \sigma(1 + \varepsilon + h\varepsilon))^2}{\sigma^3}.
\end{aligned}$$

The characteristic equation of the linearized part of (3.14) computed at $(0, 0)$ is

$$\xi^2 - \alpha_1(\varepsilon)\xi + \alpha_2(\varepsilon) = 0, \tag{3.15}$$

where

$$\alpha_1(\varepsilon) = 2 + \frac{\kappa(-1+\sigma)(1+h)^2}{\sigma},\ \alpha_2(\varepsilon) = 1 + (-1+\sigma)(1+h)^2\varepsilon.$$

The solutions of (3.15) are given by

$$\xi_{1,2} = \frac{\alpha_1(\varepsilon)}{2} \pm \frac{i}{2}\sqrt{4\alpha_2(\varepsilon) - \alpha_1^2(\varepsilon)}. \tag{3.16}$$

We then obtain $|\xi_{1,2}| = \sqrt{\alpha_2(\varepsilon)}$. Since $\sigma < 1$, then

$$\left(\frac{d|\xi_1|}{d\varepsilon}\right)_{\varepsilon=0} = \left(\frac{d|\xi_2|}{d\varepsilon}\right)_{\varepsilon=0} = -\frac{1}{2}(1-\sigma)(1+h)^2 < 0.$$

Moreover, it is necessary that $\xi_{1,2}^i \neq 1$ when $\varepsilon = 0$ for $i = 1, 2, 3, 4$, which is equivalent to $\alpha_1(0) \neq -2, 0, 1, 2$. Through simple computations, we obtain

$$\alpha_1(0) = 2 - \frac{\kappa(1-\sigma)(1+h)^2}{\sigma}.$$

Clearly, $\alpha_1(0) \neq 2$. Thus, we only require that

$$\kappa \neq \frac{4\sigma}{(1-\sigma)(1+h)^2}, \frac{2\sigma}{(1-\sigma)(1+h)^2}, \frac{\sigma}{(1-\sigma)(1+h)^2}. \tag{3.17}$$

To determine the canonical form of (3.14) at $\varepsilon = 0$, we employ the map

$$\begin{bmatrix} u_n \\ v_n \end{bmatrix} = \begin{bmatrix} \frac{(-1+\sigma)(1+h)(\sigma+\kappa(-2+\sigma)(1+h))}{\sigma^2} & 0 \\ -\frac{\kappa(-1+\sigma)(1+h)^2}{2\sigma} & -\frac{1}{2}\sqrt{4-(2+\frac{\kappa(-1+\sigma)(1+h)^2}{\sigma})^2} \end{bmatrix} \begin{bmatrix} e_n \\ f_n \end{bmatrix}. \tag{3.18}$$

After applying the map (3.18), the system (3.14) converts to

$$\begin{bmatrix} e_{n+1} \\ f_{n+1} \end{bmatrix} = \begin{bmatrix} 1 + \frac{\kappa(-1+\sigma)(1+h)^2}{2\sigma} & -\frac{1}{2}\sqrt{4-(2+\frac{\kappa(-1+\sigma)(1+h)^2}{\sigma})^2} \\ \frac{1}{2}\sqrt{4-(2+\frac{\kappa(-1+\sigma)(1+h)^2}{\sigma})^2} & 1 + \frac{\kappa(-1+\sigma)(1+h)^2}{2\sigma} \end{bmatrix} \begin{bmatrix} e_n \\ f_n \end{bmatrix} + \begin{bmatrix} \chi(e_n, f_n) \\ \Upsilon(e_n, f_n) \end{bmatrix}, \tag{3.19}$$

where

$$\begin{aligned}
\chi(e_n, f_n) &= c_1 e_n^2 + c_2 f_n^2 + c_3 e_n f_n + c_4 e_n^3 + c_5 f_n^3 + c_6 e_n^2 f_n + c_7 e_n f_n^2 + O(4), \\
\Upsilon(e_n, f_n) &= d_1 e_n^2 + d_2 f_n^2 + d_3 e_n f_n + d_4 e_n^3 + d_5 f_n^3 + d_6 e_n^2 f_n + d_7 e_n f_n^2 + O(4), \\
c_1 &= -\frac{\kappa(-1+\sigma)(1+h)^3(\sigma+\kappa(-2+\sigma)(1+h))(2\sigma+\kappa(-1+\sigma)(1+h))}{4\sigma^3}, \\
c_2 &= -\frac{(\sigma+\kappa(-2+\sigma)(1+h))(4-(2+\frac{\kappa(-1+\sigma)(1+h)^2}{\sigma})^2)}{4\sigma},
\end{aligned}$$

$$
\begin{aligned}
c_3 &= \frac{(1+h)(\sigma+\kappa(-2+\sigma)(1+h))(\sigma+\kappa(-1+\sigma)(1+h))\sqrt{4-(2+\frac{\kappa(-1+\sigma)(1+h)^2}{\sigma})^2}}{2\sigma^2},\\
c_4 &= \frac{\kappa^2(-1+\sigma)^2(1+h)^5(\sigma+\kappa(-2+\sigma)(1+h))^2(2\sigma+\kappa(-1+\sigma)(1+h))}{8\sigma^5},\\
c_5 &= -\frac{(\sigma+\kappa(-2+\sigma)(1+h))^2(4-(2+\frac{\kappa(-1+\sigma)(1+h)^2}{\sigma})^2)^{3/2}}{8\sigma^2},\\
c_6 &= -\frac{\kappa(\sigma-1)(1+h)^3(\sigma+\kappa(\sigma-2)(1+h))^2(4\sigma+3\kappa(\sigma-1)(1+h))\sqrt{4-(2+\frac{\kappa(\sigma-1)(1+h)^2}{\sigma})^2}}{8\sigma^4},\\
c_7 &= -\frac{\kappa(\sigma-1)(1+h)^3(\sigma+\kappa(\sigma-2)(1+h))^2(8\sigma^2+3\kappa^2(\sigma-1)^2(1+h)^3+2\kappa(\sigma-1)\sigma(7+8h+h^2))}{8\sigma^5},\\
d_1 &= \frac{\kappa(-1+\sigma)^2(1+h)^3(\sigma+\kappa(-2+\sigma)(1+h))(4\sigma^2+2\kappa\sigma(1+h)^2+\kappa^2(-1+\sigma)(1+h)^3)}{4\sigma^4\sqrt{4-(2+\frac{\kappa(-1+\sigma)(1+h)^2}{\sigma})^2}},\\
d_2 &= \frac{\kappa(-1+\sigma)(1+h)^2(\sigma+\kappa(-2+\sigma)(1+h))\sqrt{4-(2+\frac{\kappa(-1+\sigma)(1+h)^2}{\sigma})^2}}{4\sigma^2},\\
d_3 &= \frac{(-1+\sigma)(1+h)(\sigma+\kappa(-2+\sigma)(1+h))(2\sigma^2-\kappa\sigma(1+h)^2-\kappa^2(-1+\sigma)(1+h)^3)}{2\sigma^3},\\
d_4 &= -\frac{\kappa^3(-1+\sigma)^3(1+h)^7(\sigma+\kappa(-2+\sigma)(1+h))^2(2\sigma+\kappa(-1+\sigma)(1+h))}{8\sigma^6\sqrt{4-(2+\frac{\kappa(-1+\sigma)(1+h)^2}{\sigma})^2}},\\
d_5 &= -\frac{\kappa^2(-1+\sigma)^2(1+h)^4(\sigma+\kappa(-2+\sigma)(1+h))^2(4\sigma+\kappa(-1+\sigma)(1+h)^2)}{8\sigma^5},\\
d_6 &= \frac{\kappa^2(-1+\sigma)^2(1+h)^5(\sigma+\kappa(-2+\sigma)(1+h))^2(4\sigma+3\kappa(-1+\sigma)(1+h))}{8\sigma^5},\\
d_7 &= \frac{\kappa^2(\sigma-1)^2(1+h)^5(\sigma+\kappa(\sigma-2)(1+h))^2(8\sigma^2+3\kappa^2(\sigma-1)^2(1+h)^3+2\kappa(\sigma-1)\sigma(7+8h+h^2))}{8\sigma^6\sqrt{4-(2+\frac{\kappa(\sigma-1)(1+h)^2}{\sigma})^2}}.
\end{aligned}
$$

In order to investigate the direction of the NS bifurcation, we consider the first Lyapunov exponent, which is derived as follows:

$$
L = \left(\left[-Re\left(\frac{(1-2\xi_1)\xi_2^2}{1-\xi_1}\tau_{20}\tau_{11}\right)-\frac{1}{2}|\tau_{11}|^2-|\tau_{02}|^2+Re(\xi_2\tau_{21})\right]\right)_{\varepsilon=0}, \tag{3.20}
$$

where

$$
\begin{aligned}
\tau_{20} &= \frac{1}{8}\left[\chi_{e_ne_n}-\chi_{f_nf_n}+2\Upsilon_{e_nf_n}+i(\Upsilon_{e_ne_n}-\Upsilon_{f_nf_n}-2\chi_{e_nf_n})\right],\\
\tau_{11} &= \frac{1}{4}\left[\chi_{e_ne_n}+\chi_{f_nf_n}+i(\Upsilon_{e_ne_n}+\Upsilon_{f_nf_n})\right],\\
\tau_{02} &= \frac{1}{8}\left[\chi_{e_ne_n}-\chi_{f_nf_n}-2\Upsilon_{e_nf_n}+i(\Upsilon_{e_ne_n}-\Upsilon_{f_nf_n}+2\chi_{e_nf_n})\right],\\
\tau_{21} &= \frac{1}{16}\left[\chi_{e_ne_ne_n}+\chi_{e_nf_nf_n}+\Upsilon_{e_ne_nf_n}+\Upsilon_{f_nf_nf_n}+i(\Upsilon_{e_ne_ne_n}+\Upsilon_{e_nf_nf_n}-\chi_{e_ne_nf_n}-\chi_{f_nf_nf_n})\right].
\end{aligned}
$$

Based on the aforementioned study, the following conclusion can be drawn:

**Theorem 3.3.** *Assume that condition (5) of Theorem 2.6 is fulfilled. If condition* (3.17) *is satisfied and $L$ presented in* (3.20) *is nonzero, then* (1.2) *undergoes NS bifurcation at $E_2$ when the parameter $r$ varies in a small neighborhood of $R_2 = \frac{1}{\sigma(1+h)}(\sigma + \kappa\sigma + \kappa\sigma h - 2\kappa - 2\kappa h)$. Furthermore, if $L < 0$ (or $L > 0$), the NS bifurcation at $E_2$ is classified as supercritical (or subcritical), and a single closed invariant curve bifurcates from $E_2$, which is attracting (or repelling).*

The result shows that small changes in environmental or biological conditions may generate significant changes in plant-herbivore population dynamics, resulting in an NS bifurcation. This indicates that the system shifts from steady-state oscillations to quasiperiodic oscillations, in which populations no longer follow simple cycles but instead show increasingly complicated and interconnected patterns.

## 4. Numerical examples

The purpose of this section is to verify our theoretical results through numerical simulations. Calculations are done using MATHEMATICA, while MATLAB is used for plotting graphs.

### *4.1. Stability and bifurcation analysis varying r*

Assume that $h = 0.15, \kappa = 0.01, \sigma = 0.04$ and $x_0 = 23.4, y_0 = 0.4$. For these parametric values, the boundary FP, $E_1$, is obtained as $(24, 0)$. The system (1.2) experiences TC bifurcation at $E_1$ when $r \approx 0.629565$. The eigenvalues of $J(E_1)$ are $\xi_1 = 1$ and $\xi_2 = 0.6826$. Moreover, some careful calculations give

$$\omega(e_n, \varepsilon) = e_n - 0.039995e_n^2 - 0.0050397e_n^3 - 4e_n\varepsilon - 0.56756e_n^2\varepsilon.$$
$$\omega(0,0) = 0,\ \omega_{e_n}(0,0) = 1,\ \omega_\varepsilon(0,0) = 0,$$
$$\omega_{e_n e_n}(0,0) = -0.0799899 \neq 0,\ \omega_{e_n\varepsilon}(0,0) = -4 \neq 0.$$

It verifies Theorem 3.1. We present phase portraits in Figure 1 to graphically verify the TC bifurcation at $E_1$. Figure 1a illustrates that $E_1$ is unstable while $E_2$ is stable. In Figure 1b, it is shown that $E_1$ and $E_2$ collide at the critical value $r = 0.629565$ and, subsequently, they exchange stability. By choosing $r = 0.65$, Figure 1c demonstrates that $E_1$ becomes stable while $E_2$ turns unstable. This phenomenon is known as TC bifurcation.

Our modified system (1.2) is a generalization of the system (1.1) studied in [11]. We can obtain the original system (1.1) by substituting $h = 0$ into the modified system (1.2). In this analysis, we consider the same parameter values $\kappa = 0.01, \sigma = 0.04$ and initial conditions $x_0 = 23.4, y_0 = 0.4$, which were used in [11]. Moreover, we assume that $h = 0.15$. We vary $r$ in a bigger interval $[0.2, 0.9]$ instead of $[0.2, 0.7]$ to address additional important dynamics that are not reported in the numerical analysis presented in [11]. Our investigation shows that harvesting is helpful in stabilizing the plant-herbivore system. The system (1.2) undergoes NS bifurcation for $r \approx 0.379565$ at FP $E_2 = (24, 0.658648)$. The eigenvalues of $J(E_2)$ are $\xi_{1,2} = 0.8413 \pm 0.540569i$ with $|\xi_{1,2}| = 1$. Moreover, some careful calculations give

$$\tau_{20} = -0.0569996 + 0.0006557i, \tau_{11} = -0.0294408 + 0.0620942i,$$

$$\tau_{02} = 0.15511 + 0.0988851i, \tau_{21} = 0.006887 + 0.0094604i.$$

Thus, it is obtained that $L = -0.016401 < 0$, which verifies Theorem 3.3. Thus, NS bifurcation is supercritical, and a closed invariant attracting curve will emerge from $E_2$. Bifurcation diagrams are depicted in Figures 2a and 2b. These illustrate that $r$ stabilizes the system (1.2). The corresponding maximum Lyapunov exponent (MLE) graph is given in Figure 2c.

**(a)** $r = 0.62$

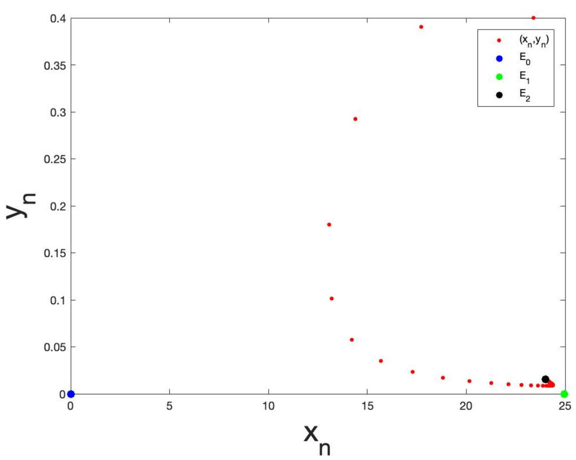


**(b)** $r = 0.629565$

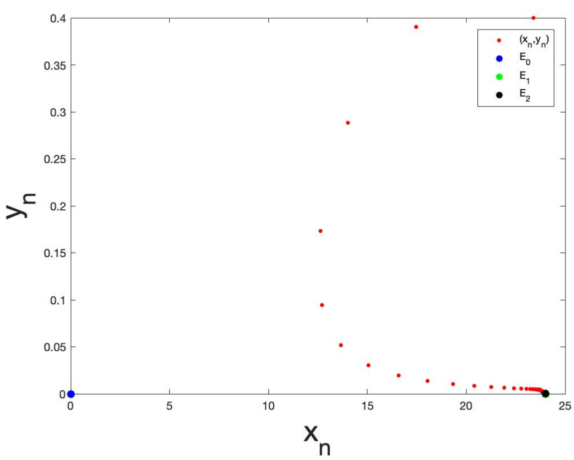


**(c)** $r = 0.65$

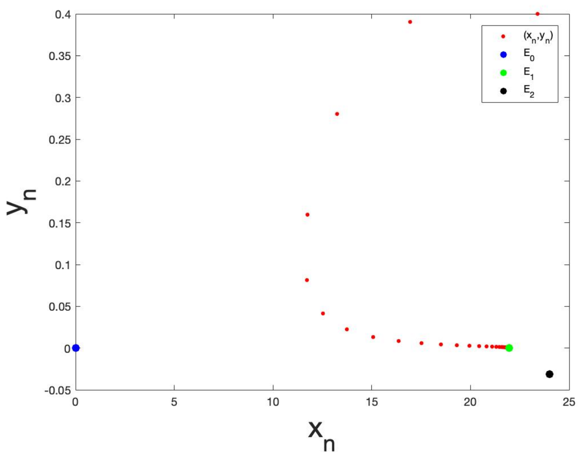


**Figure 1.** Phase portraits of system (1.2) for some values of $r$. Fixed parameter values are $h = 0.15, \kappa = 0.01, \sigma = 0.04$, and initial conditions are $x_0 = 23.4, y_0 = 0.4$.

**(a)** NS bifurcation diagram for $x_n$

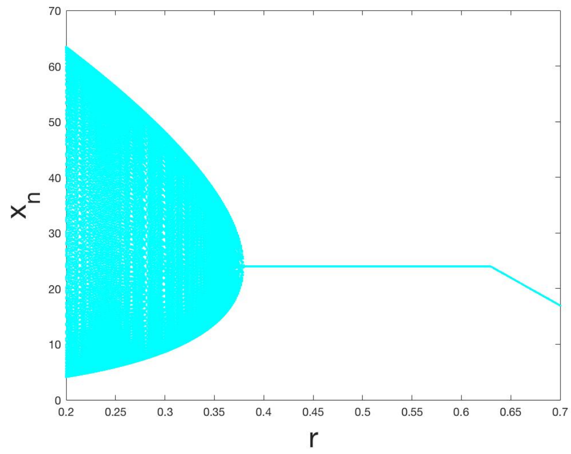


**(b)** NS bifurcation diagram for $y_n$

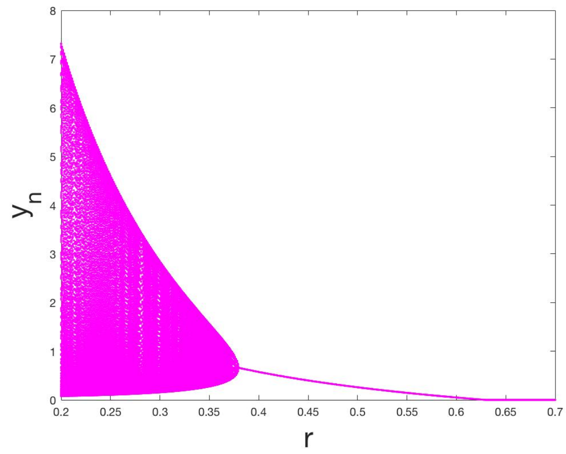


**(c)** MLE graph

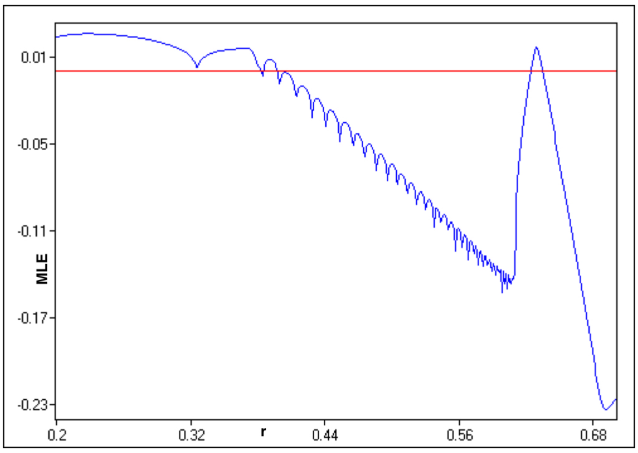


**Figure 2.** Bifurcation diagrams and MLE graph of system (1.2) varying $r$. Fixed parameter values are $h = 0.15, \kappa = 0.01, \sigma = 0.04$, and initial conditions are $x_0 = 23.4, y_0 = 0.4$.

Next, Figure 3 shows phase portraits of (1.2) for different values of $r$. It can be seen that $E_2$ is a sink for $r > 0.379565$, yet it becomes unstable at $r \approx 0.379565$ due to the occurrence of NS bifurcation. For $r \leq 0.379565$, an invariant curve emanates from $E_2$, with its radius expanding as $r$ is decreasing.

In [11], for the same parametric values and initial conditions, the positive FP is a sink for $0.51 < r < 0.76$. Their investigation shows that the system experiences NS bifurcation at $r \approx 0.51$. Although it is not highlighted in their paper, positive FP vanishes at $r \approx 0.76$ and a boundary FP appears due to TC bifurcation at the boundary FP. Later, this boundary FP also disappears for $r \geq 1$ and the system has only a trivial FP, $E_0$, which is then stable for $r > 1$. The same phenomenon is observed in our modified system (1.2). By adding the harvesting effect, the positive FP of the modified system (1.2) is a sink for $0.379565 < r < 0.629565$. The system experiences NS bifurcation at positive FP, $E_2$, for $r \approx 0.379565$. The positive FP $E_2$ disappears for $r \geq 0.629565$. The system (1.2) is experiencing TC bifurcation at boundary FP $E_1$ for $r \approx 0.629565$. Before $r \approx 0.629565$, $E_2$ is the only nontrivial FP, which is a sink for $0.379565 < r < 0.629565$. After $r \approx 0.629565$, $E_1$ is the only nontrivial FP, which is a sink for $0.629565 < r < 0.869565$. Later, the boundary FP $E_1$ also disappears for $r \geq 0.869565$. The system (1.2) is experiencing TC bifurcation at trivial FP $E_0$ for $r \approx 0.869565$. For $0.629565 < r < 0.869565$, the system possesses one boundary FP $E_1$ and one trivial FP $E_0$. Here, $E_1$ is stable, but $E_0$ is unstable. For $r > 0.869565$, the boundary FP, $E_1$, disappears, but the trivial FP $E_0$ exists, and it also becomes stable.

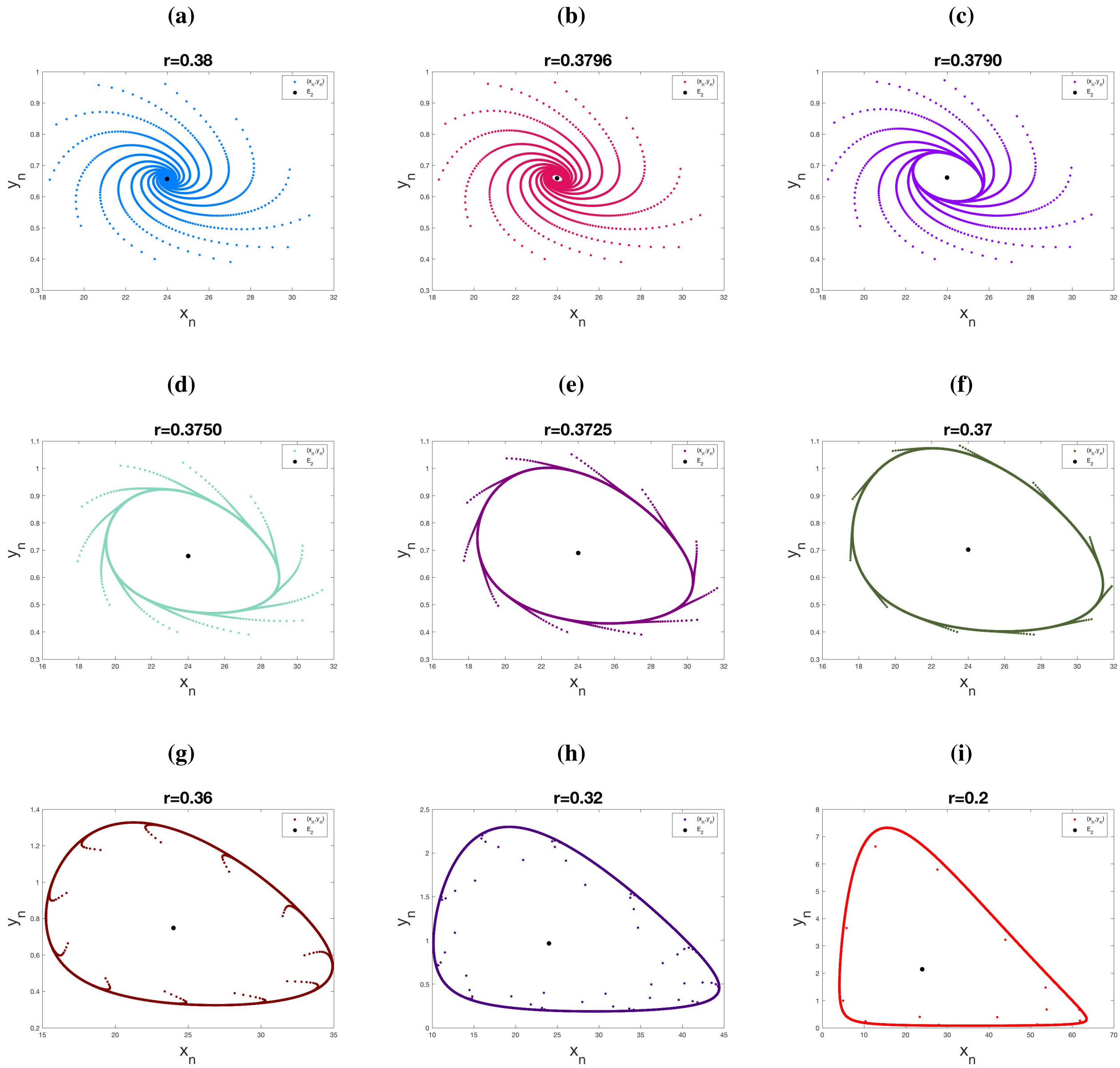


**Figure 3.** Phase portraits of (1.2) for different values of $r$ and using $h = 0.15, \kappa = 0.01, \sigma = 0.04, x_0 = 23.4, y_0 = 0.4$.

### *4.2. Stability and bifurcation analysis varying h*

In the previous section, it was shown that the harvesting effect has a stabilizing impact on plant-herbivore systems. One natural question arises: What will happen if we harvest without any set upper and lower limits? Will it still stabilize the system or destabilize if we significantly increase or decrease the harvesting limit? Ecologically, threshold harvesting is beneficial for both plants and herbivores. In this numerical analysis, it is shown that a balanced amount of harvesting is advantageous for both plants and herbivores. For this purpose, assume that $r = 0.022, \kappa = 0.01, \sigma = 0.5$, and vary $h$. For these parametric values, the NS bifurcation value is $h_1 = 18.2308$ and the PD bifurcation value is $h_2 = 18.5673$. The FP $E_2$ is a sink if $18.2308 < h < 18.5673$. The FP $E_2$ becomes unstable for $h \leq 18.2308$ due to NS bifurcation. Moreover, it is unstable for $h \geq 18.5673$ due to NS bifurcation.

The positive FP is obtained as $E_2 = (1, 0.909091)$ for $h = h_1$. The eigenvalues of $J(E_2)$ are $\xi_{1,2} = -0.849112 \pm 0.528212i$ with $|\xi_{1,2}| = 1$. Moreover, some careful calculations give

$$\tau_{20} = 5.44983 + 14.6964i, \tau_{11} = 6.73996 + 30.7151i,$$
$$\tau_{02} = 1.40817 + 16.4319i, \tau_{21} = 4.7593 + 13.5547i.$$

Thus, it is obtained that $L = -93.568 < 0$, which verifies Theorem 3.3. Thus, NS bifurcation is supercritical, and a closed invariant attracting curve will emerge from $E_2$. The bifurcation diagrams of system (1.2) are given in Figures 4a and 4b by using initial conditions $x_0 = 1.1, y_0 = 0.9$, and varying $h$ in $[18.20, 18.30]$. The corresponding MLE graph is given in Figure 4e. Next, the positive FP is obtained as $E_2 = (1, 0.86844)$ for $h = h_2$. The eigenvalues of $J(E_2)$ are $\xi_1 = -1$ and $\xi_2 = -0.828791$. Moreover, some careful calculations give $l_1 = -10.6168 \neq 0$ and $l_2 = 6.90668 \neq 0$, which verifies Theorem 3.2. Since $l_2 > 0$, a stable orbit of period-2 emanates from $E_2$. The bifurcation diagrams are given in Figures 4c and 4d by using initial conditions $x_0 = 1.1, y_0 = 0.85$, and varying $h$ in $[18.50, 18.65]$. The corresponding MLE graph is given in Figure 4f. Figures depict phase portraits of (1.2) for different values of $r$. These illustrate that $E_2$ is a sink if $18.2308 < h < 18.5673$. The system undergoes NS bifurcation at $h \approx 18.2308$ and PD bifurcation at $h \approx 18.5673$.

Figures 4 and 5 illustrate that the higher or lower harvesting effect destabilizes the system, resulting in more complicated dynamical behaviors. Thus, a balanced amount of harvesting is advantageous for both plants and herbivores. Ecologically, under moderate harvesting, there is a stable coexistence of both plants and herbivores, represented by the positive FP. As harvesting increases, herbivores struggle to find food, eventually leading to extinction. Continued harvesting eventually causes the plant population to decline as well, resulting in the extinction of plants. This indicates that moderate harvesting can sustain both populations, but excessive harvesting leads to the collapse of the entire ecosystem.

**(a)** NS bifurcation diagram for $x_n$

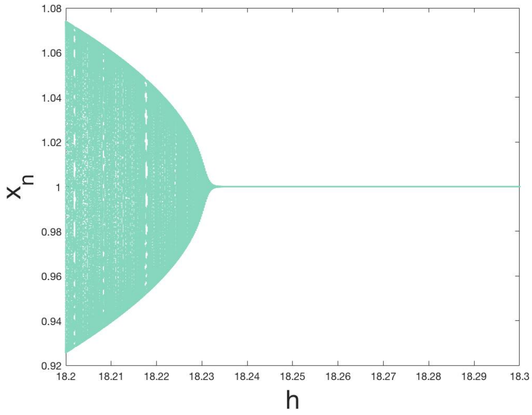


**(b)** NS bifurcation diagram for $y_n$

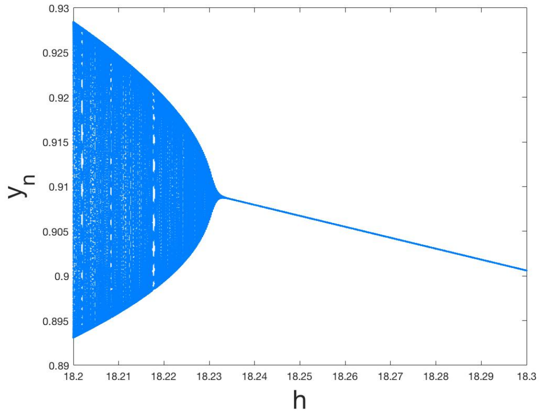


**(c)** PD bifurcation diagram for $x_n$

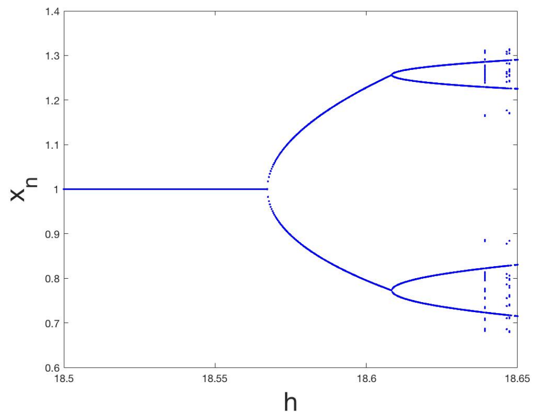


**(d)** PD bifurcation diagram for $y_n$

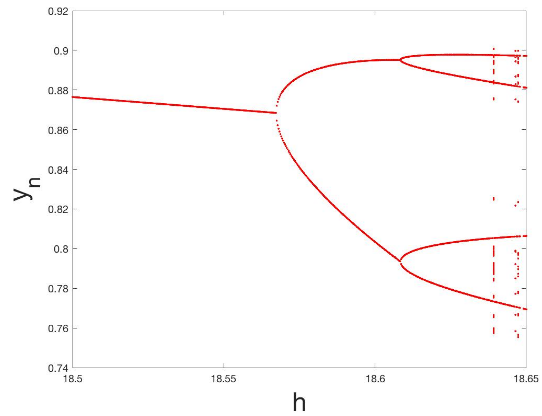


**(e)** MLE graph for NS bifurcation

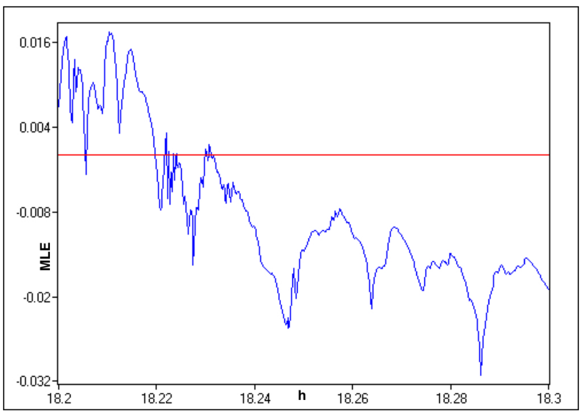


**(f)** MLE graph for PD bifurcation

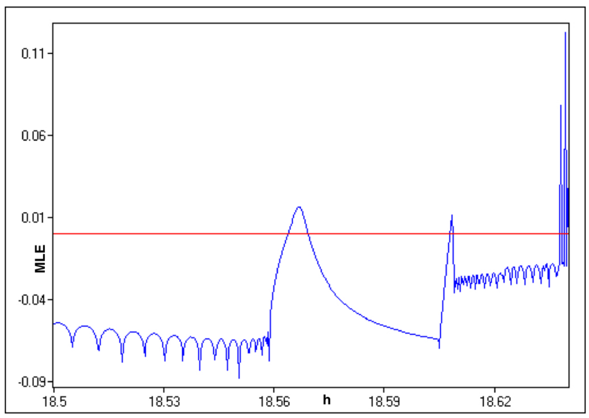


**Figure 4.** Bifurcation diagrams and MLE graphs of system (1.2) varying $h$ and fixing $r = 0.022, \kappa = 0.01, \sigma = 0.5$. The initial conditions are (a,b, e) $x_0 = 1.1, y_0 = 0.9$, (c, d, f) $x_0 = 1.1, y_0 = 0.85$.

**(a)** $r = 18.20$

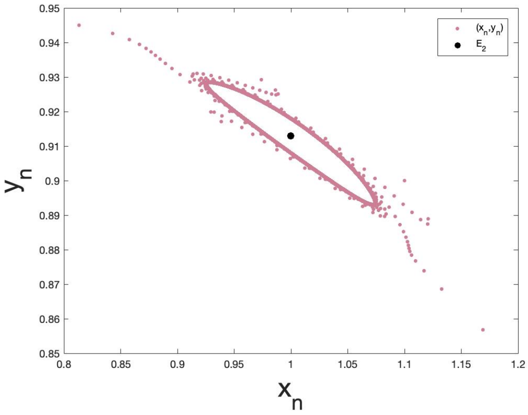


**(b)** $r = 18.22$

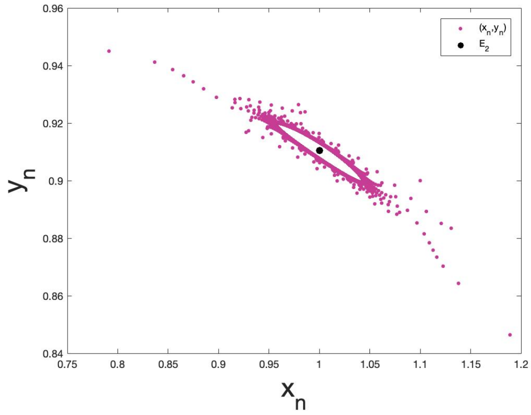


**(c)** $r = 18.24$

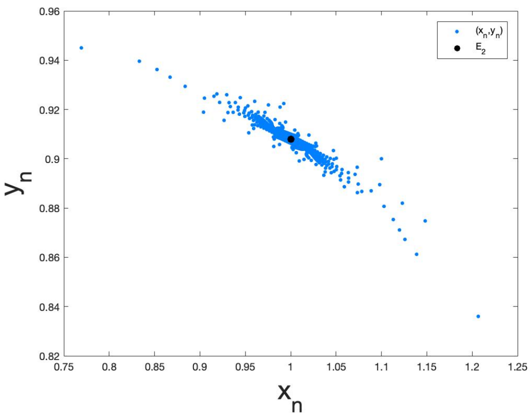


**(d)** $r = 18.56$

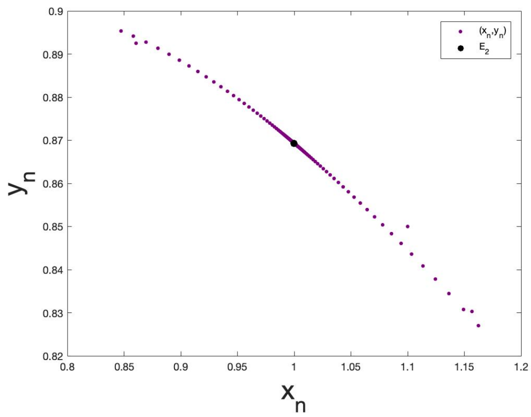


**(e)** $r = 18.57$

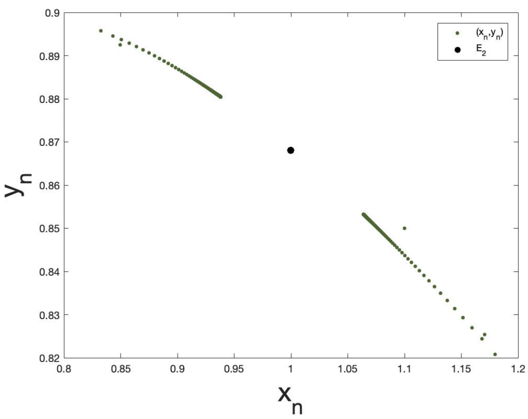


**(f)** $r = 18.66$

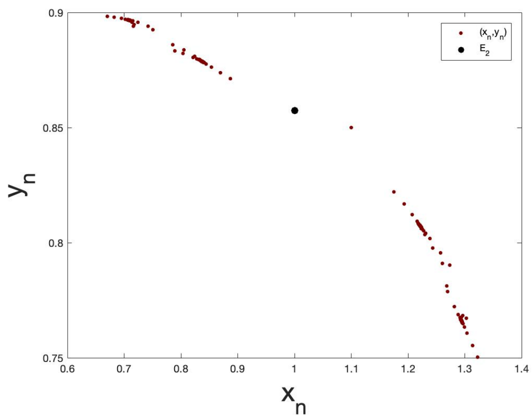


**Figure 5.** Phase portraits of system (1.2) for some values of $r$ and fixing $r = 0.022, \kappa = 0.01, \sigma = 0.5$. The initial conditions are (a-c) $x_0 = 1.1, y_0 = 0.9$, (d-f) $x_0 = 1.1, y_0 = 0.85$.

## 5. Influence of harvesting effect

The aim of this section is to investigate the influence of the harvesting effect on the dynamics of system (1.2). Incorporating a harvesting effect into a plant-herbivore system yields insightful findings that underscore the intricate dynamics of species interactions in ecological systems. While the harvesting effect is directly applied to the plant population, its influence extends beyond that, indirectly impacting herbivore dynamics through the interaction between plant and herbivore populations. One can observe in Figure 4 that system (1.2) undergoes PD and NS bifurcations at the positive FP $E_2$ by varying the harvesting effect parameter $h$. These show that the harvesting effect can stabilize or destabilize the system. Notably, a moderate level of the harvesting effect appears to be advantageous for both plant and herbivore populations, as evidenced by the occurrence of these bifurcations. Furthermore, the positive FP $E_2 = (x_2, y_2)$ is dependent on the harvesting effect parameter $h$. Through simple calculations, one can obtain that $\frac{dx_2}{dh} = 0$ and $\frac{dy_2}{dh} = -\frac{1}{r(1+h)^2} < 0$. Ecologically, it represents that when the harvesting effect strengthens in the plant population, it might become slightly more difficult for herbivores to survive. A decrease in plant availability could lead to reduced reproduction rates or increased mortality among herbivores, ultimately resulting in a decrease in the population growth rate of herbivores.

## 6. Conclusions

This study explores the implications of adding a harvesting impact to the dynamics of a plant-herbivore system. Our findings highlight the intricate interplay between species interactions in ecological systems, emphasizing the significance of the harvesting effect. The harvesting effect affects the plant population directly, but it also has an impact on herbivore dynamics because of the complex interactions that occur between herbivores and plant populations. The existence and stability of FPs are examined. Furthermore, a comprehensive analysis of local bifurcations at the positive FP is conducted. The investigation reveals that the system (1.2) undergoes PD, TC, and NS bifurcations. These bifurcations demonstrate the system's sensitivity to small parameter changes, which result in significant changes in population dynamics. The role of transcritical bifurcation is to emphasize the critical transition from coexistence to dominance of plant populations; PD bifurcations show the formation of complex oscillatory patterns. NS bifurcations, in turn, indicate the transition from steady-state to quasiperiodic oscillations, displaying the complexity and adaptability of ecological interactions.

The plant-herbivore system without harvesting effect was investigated in [11]. Our plant-herbivore system is more general, and we can obtain the results of [11] by just replacing $h = 0$ into our results. Although we obtain similar results as in [11], the following are the main differences observed in both plant-herbivore systems:

- With the same parametric values and initial conditions, the positive FP of system (1.1) is a sink inside the range $0.51 < r < 0.76$. However, when the harvesting effect is included, the positive FP of system (1.2) is a sink inside the range $0.379565 < r < 0.629565$ for $h = 0.15$. This illustrates that harvesting helps to stabilize the plant-herbivore system for lower values of $r$.
- In the absence of harvesting, the system (1.1) does not experience PD bifurcation. However, when the harvesting is added, the system (1.2) experiences PD bifurcation at the positive FP.

An interesting finding in our paper is that a moderate amount of the harvesting effect benefits both plant and herbivore populations, emphasizing the intricate impact of harvesting on ecosystem dynamics. These results have significant biological consequences, as they reveal the intricate relationship between human involvement and the capacity of ecosystems to recover. They also highlight the need to adopt sustainable harvesting methods to safeguard the long-term well-being and stability of ecological systems. In the future, one can try to investigate the global dynamics and codimension-two bifurcations for the plant-herbivore system (1.2).

## Author contributions

Mohammed Alsubhi: Formal Analysis, Validation, Writing-original draft, Methodology; Rizwan Ahmed: Conceptualization, Investigation, Writing-review & editing, Software, Supervision; Ibrahim Alraddadi: Conceptualization, Validation, Writing-review & editing, Visualization, Supervision, Methodology; Faisal Alsharif: Formal Analysis, Software, Visualization, Methodology; Muhammad Imran: Formal Analysis, Investigation, Writing-original draft, Software. All authors have read and approved the final version of the manuscript for publication.

## Use of AI tools declaration

The authors declare they have not used Artificial Intelligence (AI) tools in the creation of this article.

## Acknowledgments

The authors extend their appreciation to the Deputyship for Research & Innovation, Ministry of Education in Saudi Arabia for funding this research work through the project number (445-9-923).

## Conflict of interest

All authors declare no conflicts of interest in this paper.

## References

1. D. Choquenot, J. Parkes, Setting thresholds for pest control: How does pest density affect resource viability?, *Biol. Conserv.*, **99** (2001), 29–46. https://doi.org/10.1016/S0006-3207(00)00186-5
2. L. Edelstein-Keshet, Mathematical theory for plant-herbivore systems, *J. Math. Biol.*, **24** (1986), 25–58. https://doi.org/10.1007/bf00275719
3. E. P. Holland, R. P. Pech, W. A. Ruscoe, J. P. Parkes, G. Nugent, R. P. Duncan, Thresholds in plant-herbivore interactions: predicting plant mortality due to herbivore browse damage, *Oecologia*, **172** (2013), 751–766. https://doi.org/10.1007/s00442-012-2523-5
4. Z. Feng, Z. Qiu, R. Liu, D. L. DeAngelis, Dynamics of a plant-herbivore-predator system with plant-toxicity, *Math. Biosci.*, **229** (2011), 190–204. https://doi.org/10.1016/j.mbs.2010.12.005

5. K. C. Abbott, G. Dwyer, Food limitation and insect outbreaks: complex dynamics in plant-herbivore models, *J. Anim. Ecol.*, **76** (2007), 1004–1014. https://doi.org/10.1111/j.1365-2656.2007.01263.x

6. G. Sui, M. Fan, I. Loladze, Y. Kuang, The dynamics of a stoichiometric plant-herbivore model and its discrete analog, *Math. Biosci. Eng.*, **4** (2007), 29–46. https://doi.org/10.3934/mbe.2007.4.29

7. Y. Kang, D. Armbruster, Y. Kuang, Dynamics of a plant-herbivore model, *J. Biol. Dynam.*, **2** (2008), 89–101. https://doi.org/10.1080/17513750801956313

8. Q. Din, A. A. Elsadany, H. Khalil, Neimark-Sacker bifurcation and chaos control in a fractional-order plant-herbivore model, *Discrete Dyn. Nat. Soc.*, **2017** (2017), 6312964. https://doi.org/10.1155/2017/6312964

9. M. S. Khan, M. Samreen, M. Ozair, T. Hussain, E. M. Elsayed, J. F. Gomez-Aguilar, On the qualitative study of a two-trophic plant-herbivore model, *J. Math. Biol.*, **85** (2022), 34. https://doi.org/10.1007/s00285-022-01809-0

10. E. Beso, S. Kalabusic, E. Pilav, Food-limited plant-herbivore model: bifurcations, persistence, and stability, *Math. Biosci.*, **370** (2024), 109157. https://doi.org/10.1016/j.mbs.2024.109157

11. M. S. Shabbir, Q. Din, M. D. la Sen, J. F. Gómez-Aguilar, Exploring dynamics of plant-herbivore interactions: bifurcation analysis and chaos control with Holling type-II functional response, *J. Math. Biol.*, **88** (2024), 8. https://doi.org/10.1007/s00285-023-02020-5

12. Z. Feng, D. L. DeAngelis, *Mathematical models of plant-herbivore interactions*, Chapman and Hall/CRC, 2017. https://doi.org/10.1201/9781315154138

13. S. Kartal, A. Debbouche, Dynamics of a plant-herbivore model with differential-difference equations, *Cogent Mathematics*, **3** (2016), 1136198. https://doi.org/10.1080/23311835.2015.1136198

14. E. Beso, S. Kalabusic, E. Pilav, A. Bilgin, Dynamics of a plant-herbivore model subject to Allee effects with logistic growth of plant biomass, *Int. J. Bifurcat. Chaos*, **33** (2023), 2330026. https://doi.org/10.1142/s0218127423300264

15. Q. Din, Global behavior of a plant-herbivore model, *Adv. Differ. Equ.*, **2015** (2015), 119. https://doi.org/10.1186/s13662-015-0458-y

16. A. Q. Khan, J. Ma, D. Xiao, Bifurcations of a two-dimensional discrete time plant-herbivore system, *Commun. Nonlinear Sci.*, **39** (2016), 185–198. https://doi.org/10.1016/j.cnsns.2016.02.037

17. M. Y. Hamada, Dynamical analysis of a discrete-time plant-herbivore model, *Arab. J. Math.*, **13** (2024), 121–131. https://doi.org/10.1007/s40065-023-00442-z

18. T. Saha, M. Bandyopadhyay, Dynamical analysis of a plant-herbivore model bifurcation and global stability, *J. Appl. Math. Comput.*, **19** (2005), 327–344. https://doi.org/10.1007/bf02935808

19. Y. Li, Z. Feng, R. Swihart, J. Bryant, N. Huntly, Modeling the impact of plant toxicity on plant-herbivore dynamics, *J. Dyn. Diff. Equat.*, **18** (2006), 1021–1042. https://doi.org/10.1007/s10884-006-9029-y

20. C. Castillo-Chavez, Z. Feng, W. Huang, Global dynamics of a plant-herbivore model with toxin-determined functional response, *SIAM J. Appl. Math.*, **72** (2012), 1002–1020. https://doi.org/10.1137/110851614

21. E. M. Elsayed, Q. Din, Period-doubling and Neimark-Sacker bifurcations of plant-herbivore models, *Adv. Differ. Equ.*, **2019** (2019), 271. https://doi.org/10.1186/s13662-019-2200-7
22. Q. Din, M. S. Shabbir, M. A. Khan, K. Ahmad, Bifurcation analysis and chaos control for a plant-herbivore model with weak predator functional response, *J. Biol. Dynam.*, **13** (2019), 481–501. https://doi.org/10.1080/17513758.2019.1638976
23. S. Kalabusic, E. Pilav, Bifurcations, permanence and local behavior of the plant-herbivore model with logistic growth of plant biomass, *Qual. Theory Dyn. Syst.*, **21** (2022), 26. https://doi.org/10.1007/s12346-022-00561-6
24. L. J. Allen, M. J. Strauss, H. G. Thorvilson, W. N. Lipe, A preliminary mathematical model of the apple twig borer (Coleoptera: Bostrichidae) and grapes on the texas high plains, *Ecol. Model.*, **58** (1991), 369–382. https://doi.org/10.1016/0304-3800(91)90046-4
25. L. J. Allen, M. K. Hannigan, M. J. Strauss, Mathematical analysis of a model for a plant-herbivore system, *Bull. Math. Biol.*, **55** (1993), 847–864. https://doi.org/10.1016/S0092-8240(05)80192-2
26. H. P. Benoit, D. P. Swain, Impacts of environmental change and direct and indirect harvesting effects on the dynamics of a marine fish community, *Can. J. Fish. Aquat. Sci.*, **65** (2008), 2088–2104. https://doi.org/10.1139/f08-112
27. S. A. Khamis, J. M. Tchuenche, M. Lukka, M. Heilio, Dynamics of fisheries with prey reserve and harvesting, *Int. J. Comput. Math.*, **88** (2011), 1776–1802. https://doi.org/10.1080/00207160.2010.527001
28. C. K. Yosi, R. J. Keenan, J. C. Fox, Forest dynamics after selective timber harvesting in Papua New Guinea, *Forest Ecol. Manag.*, **262** (2011), 895–905. https://doi.org/10.1016/j.foreco.2011.06.007
29. D. N. Rasquinha, D. R. Mishra, Impact of wood harvesting on mangrove forest structure, composition and biomass dynamics in india, *Estuar. Coast. Shelf Sci.*, **248** (2021), 106974. https://doi.org/10.1016/j.ecss.2020.106974
30. R. Ahmed, Complex dynamics of a fractional-order predator-prey interaction with harvesting, *Open Journal of Discrete Applied Mathematics*, **3** (2020), 24–32. https://doi.org/10.30538/psrp-odam2020.0040
31. Y. Tian, H. M. Li, The study of a predator-prey model with fear effect based on state-dependent harvesting strategy, *Complexity*, **2022** (2022), 9496599. https://doi.org/10.1155/2022/9496599
32. M. Imran, M. B. Almatrafi, R. Ahmed, Stability and bifurcation analysis of a discrete predator-prey system of Ricker type with harvesting effect, *Commun. Math. Biol. Neurosci.*, **2024** (2024), 11. https://doi.org/10.28919/cmbn/8313
33. M. Virtala, Optimal harvesting of a plant-hervibore system: lichen and reindeer in northern Finland, *Ecol. Model.*, **60** (1992), 233–255. https://doi.org/10.1016/0304-3800(92)90035-d
34. M. D. Asfaw, S. M. Kassa, E. M. Lungu, Co-existence thresholds in the dynamics of the plant-herbivore interaction with Allee effect and harvest, *Int. J. Biomath.*, **11** (2018), 1850057. https://doi.org/10.1142/s1793524518500572
35. M. Xiao, J. Cao, Hopf bifurcation and non-hyperbolic equilibrium in a ratio-dependent predator-prey model with linear harvesting rate: analysis and computation, *Math. Comput. Model.*, **50** (2009), 360–379. https://doi.org/10.1016/j.mcm.2009.04.018

36. L. Ji, C. Wu, Qualitative analysis of a predator-prey model with constant-rate prey harvesting incorporating a constant prey refuge, *Nonlinear Anal.-Real*, **11** (2010), 2285–2295. https://doi.org/10.1016/j.nonrwa.2009.07.003
37. D. Jana, R. Agrawal, R. K. Upadhyay, G. Samanta, Ecological dynamics of age selective harvesting of fish population: maximum sustainable yield and its control strategy, *Chaos Soliton. Fract.*, **93** (2016), 111–122. https://doi.org/10.1016/j.chaos.2016.09.021
38. A. Xiao, C. Lei, Dynamic behaviors of a non-selective harvesting single species stage-structured system incorporating partial closure for the populations, *Adv. Differ. Equ.*, **2018** (2018), 245. https://doi.org/10.1186/s13662-018-1709-5
39. L. J. S. Allen, *An introduction to mathematical biology*, Pearson/Prentice Hall, 2007.
40. Q. Din, Neimark-Sacker bifurcation and chaos control in Hassell-Varley model, *J. Differ. Equ. Appl.*, **23** (2017), 741–762. https://doi.org/10.1080/10236198.2016.1277213
41. Q. Din, M. I. Khan, A discrete-time model for consumer-resource interaction with stability, bifurcation and chaos control, *Qual. Theor. Dyn. Syst.*, **20** (2021), 56. https://doi.org/10.1007/s12346-021-00488-4
42. A. A. Khabyah, R. Ahmed, M. S. Akram, S. Akhtar, Stability, bifurcation, and chaos control in a discrete predator-prey model with strong Allee effect, *AIMS Mathematics*, **8** (2023), 8060–8081. https://doi.org/10.3934/math.2023408
43. R. Ahmed, M. B. Almatrafi, Complex dynamics of a predator-prey system with Gompertz growth and herd behavior, *Int. J. Anal. Appl.*, **21** (2023), 100. https://doi.org/10.28924/2291-8639-21-2023-100
44. R. Ahmed, M. Rafaqat, I. Siddique, M. A. Arefin, Complex dynamics and chaos control of a discrete-time predator-prey model, *Discrete Dyn. Nat. Soc.*, **2023** (2023), 8873611. https://doi.org/10.1155/2023/8873611
45. A. C. J. Luo, *Regularity and complexity in dynamical systems*, New York: Springer, 2012. https://doi.org/10.1007/978-1-4614-1524-4
46. J. Guckenheimer, P. Holmes, *Nonlinear oscillations, dynamical systems, and bifurcations of vector fields*, New York: Springer, 1983. https://doi.org/10.1007/978-1-4612-1140-2
47. S. Wiggins, *Introduction to applied nonlinear dynamical systems and chaos*, New York: Springer, 2003. https://doi.org/10.1007/b97481
48. W. Yao, X. Li, Complicate bifurcation behaviors of a discrete predator-prey model with group defense and nonlinear harvesting in prey, *Appl. Anal.*, **102** (2023), 2567–2582. https://doi.org/10.1080/00036811.2022.2030724
49. P. A. Naik, M. Amer, R. Ahmed, S. Qureshi, Z. Huang, Stability and bifurcation analysis of a discrete predator-prey system of Ricker type with refuge effect, *Math. Biosci. Eng.*, **21** (2024), 4554–4586. https://doi.org/10.3934/mbe.2024201


AIMS Press

© 2024 the Author(s), licensee AIMS Press. This is an open access article distributed under the terms of the Creative Commons Attribution License (https://creativecommons.org/licenses/by/4.0)